On the Thermodynamic Geometry and Critical Phenomena of AdS Black Holes

Anurag Sahay, Tapobrata Sarkar, Gautam Sengupta *

Department of Physics,
Indian Institute of Technology,
Kanpur 208016,
India

Abstract

In this paper, we study various aspects of the equilibrium thermodynamic state space geometry of AdS black holes. We first examine the Reissner-Nordstrom-AdS (RN-AdS) and the Kerr-AdS black holes. In this context, the state space scalar curvature of these black holes is analysed in various regions of their thermodynamic parameter space. This provides important new insights into the structure and significance of the scalar curvature. We further investigate critical phenomena, and the behaviour of the scalar curvature near criticality, for KN-AdS black holes in two mixed ensembles, introduced and elucidated in our earlier work arXiv:1002.2538 [hep-th]. The critical exponents are identical to those in the RN-AdS and Kerr-AdS cases in the canonical ensemble. This suggests an universality in the scaling behaviour near critical points of AdS black holes. Our results further highlight qualitative differences in the thermodynamic state space geometry for electric charge and angular momentum fluctuations of these.

*E-mail: ashaya, tapo, sengupta @iitk.ac.in

1 Introduction

It has been widely recognized over the past few decades that thermodynamic properties of black holes (see, e.g [1], [2], [3]) and references therein) provide an important analytical tool for understanding several issues involving quantum theories of gravity. The topic has been intensely discussed in the recent past, and several key features have been uncovered, especially in the context of black holes arising in String Theory. However, a knowledge of the exact statistical description of black hole microstates is still elusive, although thermodynamic studies of black holes do indicate extremely interesting phase structures and critical phenomena in these systems.

In particular, black holes in asymptotically anti de-Sitter space have been at the center of extensive research since the discovery of Maldacena's AdS/CFT correspondence [4]. The gauge/gravity duality is expected to play a major role in our efforts to understand the underlying microscopic statistical interactions in black holes via the gauge theory living on the boundary. For example, this duality has led to the celebrated correspondence between Hawking-Page phase transitions in asymptotically AdS black holes and confinement-deconfinement phase transitions in the boundary quantum field theory.

In a separate context, a geometrical perspective of equilibrium thermodynamics has been developed over the last few decades. As is well known, an extrinsic geometrical perspective of thermodynamics has been elucidated following early treatments by Tisza [5] and Callen [6]. However an intrinsic geometrical structure inherent in thermodynamics turned out to be much more elusive. Following the early work of Weinhold [7], in the energy representation, it was possible to define a Riemannian metric on the space of the equilibrium thermodynamic states of a system. However it was not possible to interpret this physically. In a later development Ruppeiner [8] provided an intrinsic Riemannian geometrical framework in the entropy representation for the equilibrium thermodynamic state space of a system. The line elemnt in this case could be related to the probability measure of thermodynamic fluctuations connecting two equilibrium states and has been refered to as the thermodynamic geometry of a system. The first analysis of black hole thermodynamics in the framework of thermodynamic geometry was presented in [9] for extremal black holes in supergravity theories. In the last few years the thermodynamic geometry of both extremal and non extremal black holes have been a subject of investigations and have provided interesting insights into the thermodynamics, phase transition and critical phenomena of black holes. However there are still numerous unresolved issues which merit further detailed analysis of diverse black holes in this framework.

To this end, in [10], we studied the thermodynamic geometry of Kerr-Newman-AdS (KN-AdS) black holes in the grand canonical and two novel "mixed" ensembles, wherein one of the two thermodynamic charges, (i.e the angular momentum or the electric charge), was held fixed while the other charge was allowed to be exchanged with the surroundings of black hole. For the mixed ensembles, we were able to establish new phase structures exhibiting liquid-gas like first order phase transitions culminating in a critical point. The scalar curvature, R, of the state space Riemannian geometries corresponding to these ensembles show a divergence

at the critical point analogous to that for conventional critical phenomena. Interestingly, we showed that the scalar curvature also carries information about first order phase transitions in these black hole systems. This is encoded in the multivalued branch structure of the scalar curvature in the phase coexistence regions. We examined this issue in detail, first in the context of a conventional Van der Waals model and followed it up with an extensive analysis of the mixed ensemble black holes, finding that the two systems closely resemble each other in the behaviour of their scalar curvature near first and second order phase transitions.

In the present work we complement our earlier investigation by undertaking a detailed investigation of the scaling behaviour of the thermodynamic functions and the corresponding scalar curvatures near the critical points of these black holes. For the two mixed ensembles, we calculate the critical exponents by developing a general perturbative scheme for thermodynamic quantities depending on two independent control parameters, like the temperature and the electric potential. We then compare the critical exponents with the known case of Reissner-Nordstrom-AdS (RN-AdS) black holes, as obtained in [11] and [12], and also check whether these exponents follow from a more general scaling law for the singular part of the free energy near criticality. We also obtain the scaling behaviour of R and compare it with its known critical behaviour for conventional thermodynamic systems, as explained in [8].

As regards thermodynamic geometry, it is believed that the sign of the state space scalar curvature R is an indicator of the nature of microscopic interactions undelying the thermodynamic system. For example, it was observed in the case of ideal quantum gases that R is positive for repulsive fermi interactions and negative for attractive bosonic interactions [13]. Similarly, for the case of anyon gases obeying fractional statistics, R was shown to become positive for repulsive quantum interactions and negative for attractive quantum interactions, [14]. However, a convincing physical or analytical justification for this attribute of R is still forthcoming. The issue of the sign of R becomes more pressing in the case of black holes, where it is well known that R for different black holes usually changes sign on varying the independent thermodynamic charges. Moreover, the problem is compounded by a lack of knowledge of the microscopic interactions in the case of black holes. In our previous work, we had addressed the issue of the sign of R by first obtaining a global picture of its sign variations. This was achieved by plotting its zeroes in the parameter space of fluctuating variables for various ensembles. Our approach was mainly kinematic, in the sense that the investigations were confined to observing the sign variations in R for the grand canonical and the two mixed ensembles of KN-AdS black holes, with brief comments on the differences in the various cases. Other approach, which we had studied extensively, was to adopt the view that, irrespective of its signature, the *magnitude* of the state space scalar curvature , $|R|$, is a measure of strength of interactions in the black hole, [15]. From the plots of $|R|$ vs. t we could make some interesting observations regarding the stability of small black hole branches vis. a vis the large black hole branches, which sometimes ran counter to common expectations.

In the present work we address the issue of the sign variations in R in a more systematic fashion. We start with the assertion that just as in the case of

conventional thermodynamic systems, the state space scalar curvature for black holes too is indicative of the (yet unknown) nature of microscopic interactions. In order to substantiate this viewpoint, we carefully study the scalar curvature corresponding to different kinds of thermodynamic fluctuations for black holes in AdS space. Starting with the simpler cases of RN-AdS and Kerr-AdS black holes, each of them having a two dimensional state space geometry, we move on to discuss the KN-AdS black hole in the grand canonical ensemble, which has a three dimensional state space geometry consisting of fluctuations in the mass, electric charge and the angular momentm m, q and j respectively. We then study the scalar curvature corresponding to the two dimensional state space of KN AdS black holes in the mixed ensembles. One of the main conclusions following our investigation of the different scalar curvatures is that the presence of q fluctuations always brings about a change in the sign of R, whereas the j fluctuations do not effect any such sign change.

This paper is organized as follows. In section 2 we briefly discuss the thermodynamics of KN-AdS black holes, mainly using it to establish our notations and obtain formulae of thermodynamic functions for later use, and then revisit the thermodynamics of RN-AdS black holes using our notation, mainly emphasizing on the grand canonical ensemble. Next we study the state space scalar curvature of these black holes in detail. In section 3 the Kerr-AdS black holes are subjected to a similar analysis, ending with a comparison between the scalar curvature of RN-AdS and Kerr-AdS black holes. In sections 4 and 5 respectively, the scalar curvature for KN-AdS black holes in the grand canonical ensemble and the two mixed ensembles alluded to earlier, is studied in details, starting with a discussion of their phase behaviour. Further, in section 5, the perturbative calculations for the critical exponents of these mixed ensemble black holes is undertaken. Finally, we summarize our results in section 5.

2 Thermodynamics of KN-AdS and RN-AdS Black Holes

In this section, as a warm up exercise, we will first review certain aspects of the thermodynamics of KN-AdS and RN-AdS black holes, before analyzing the geometry of their equilibrium state spaces. The main purpose of this section is to set the notations and conventions used in the rest of the paper. However, we emphasize that our formulation will be entirely in terms of thermodynamic variables, in contrast to analyses involving black holes parameters as commonly appear in the literature. In particular, subsection (2.2) contains qualitatively new analyses.

2.1 KN-AdS Black Holes

We begin with the Smarr formula for the KN-AdS black holes, which is [16],

$$M = \left[\frac{S}{4\pi} + \frac{\pi}{4S}\left(4J^2 + Q^4\right) + \frac{Q^2}{2} + \frac{J^2}{l^2} + \frac{S}{2\pi l^2}\left(Q^2 + \frac{S}{\pi} + \frac{S^2}{2\pi^2 l^2}\right)\right]^{\frac{1}{2}} \qquad (1)$$

where M is the mass of the black hole, S is the entropy and J, Q are the angular momentum and the electric charge respectively. This formula differs from that of asymptotically flat Kerr-Newman black holes in the last two terms which arise because of a finite AdS length scale. It can be verified from the Smarr formula that the mass M is a homogenous function of degree $1/2$ in S, J, Q^2 and l^2, ([16]),

$$M(\lambda S, \lambda J, \lambda Q^2, \lambda l^2) = \lambda^{1/2} M(S, J, Q^2, l^2) \tag{2}$$

where λ is a constant. Since we will not be treating the AdS length l as a thermodynamic variable, i.e we are not considering ensembles in which l may fluctuate, we absorb it into the Smarr formula by taking the scaling constant λ equal to $1/l^2$. The rescaled thermodynamic variables are then defined as

$$m = \frac{M}{l},\ s = \frac{S}{l^2},\ q = \frac{Q}{l},\ j = \frac{J}{l^2} \tag{3}$$

The Smarr formula, after the rescaling, becomes

$$m = \frac{1}{2}\left(\frac{s^4 + 2s^3\pi + s^2\pi^2\left(2q^2+1\right) + \pi^3 s\left(2q^2+4j^2\right) + \pi^2\left(q^4+4j^2\right)}{\pi^3 s}\right)^{\frac{1}{2}} \tag{4}$$

We can calculate the conjugate quantities like the temperature and potentials using the first law of thermodynamics, i.e by differentiating the Smarr formula for m with respect to the charges s, q and j.

$$dm = tds + \omega dj + \phi dq, \tag{5}$$

where the rescaled angular velocity, temperature and the electric potential are defined as

$$\omega = l\Omega\ ,\ t = lT\ ,\ \phi = \Phi \tag{6}$$

Although the expressions are standard, we reproduce some of them for convenience. The electric potential ϕ and the angular velocity ω, as functions of the charges (i.e s, q, j) are given by

$$\phi = \frac{\pi^{\frac{1}{2}} q\left(s^2 + s\pi + q^2\pi^2\right)}{s^{\frac{1}{2}}\left[s^4 + 2s^3\pi + s^2\pi^2\left(1+2q^2\right) + 2q^2\pi^3 s + 4\pi^3 j^2\left(\pi+s\right)\right]^{\frac{1}{2}}} \tag{7}$$

$$\omega = \frac{2\pi^{\frac{3}{2}} j\left(\pi+s\right)}{s^{\frac{1}{2}}\left[s^4 + 2s^3\pi + s^2\pi^2\left(1+2q^2\right) + 2q^2\pi^3 s + 4\pi^3 j^2\left(\pi+s\right)\right]^{\frac{1}{2}}} \tag{8}$$

whereas the temperature of the black hole is given by

$$t = \frac{3s^4 + 4s^3\pi + s^2\pi^2\left(1+2q^2\right) - 4\pi^4 j^2 - \pi^4 q^4}{4\pi^{\frac{3}{2}} s^{\frac{3}{2}}\left[s^4 + 2s^3\pi + s^2\pi^2\left(1+2q^2\right) + 2q^2\pi^3 s + 4\pi^3 j^2\left(\pi+s\right)\right]^{\frac{1}{2}}} \tag{9}$$

Having tabulated the basic formulae for KN-AdS black holes in terms of thermodynamic parameters, we now discuss the RN-AdS black holes.

2.2 RN-AdS Black Holes

Thermodynamic quantities for the RN-AdS black hole may be calculated by setting $j = 0$ in the expressions given in the previous subsection. We begin with the expression for the temperature,

$$t = \frac{1}{4}\left(\frac{3\,s^2 + s\pi - q^2\pi^2}{\pi^{3/2}s^{3/2}}\right) \tag{10}$$

From the expression for t we can obtain the charge at the extremal limit in terms of entropy s by

$$q_{ex}(s) = \frac{1}{\pi}\sqrt{s\,(3s + \pi)} \tag{11}$$

The electric potential is given by

$$\phi = \frac{q\sqrt{\pi}}{\sqrt{s}} \tag{12}$$

The value of ϕ obtained from thermodynamics is the potential measured at infinity with respect to the horizon, [16]. Let us also, for future reference, calculate the heat capacities and the susceptibility. The heat capacity at constant charge, denoted by c_q, is given by

$$c_q = t\left(\frac{\partial s}{\partial t}\right)_q = \frac{2s\,(3\,s^2 + s\pi - q^2\pi^2)}{3\,s^2 - s\pi + 3\,q^2\pi^2} \tag{13}$$

and the heat capacity at constant potential, c_ϕ is given by

$$c_\phi = t\left(\frac{\partial s}{\partial t}\right)_\phi = \frac{2s\,(3\,s^2 + s\pi - q^2\pi^2)}{3\,s^2 - s\pi + q^2\pi^2} \tag{14}$$

It can be seen that both the heat capacities vanish at extremality. The "capacitance" or the isothermal susceptibility,

$$\chi_t = \left(\frac{\partial q}{\partial \phi}\right)_t = \frac{(3\,s^2 - s\,\pi + 3\,\pi^2 q^2)\,\sqrt{s}}{\sqrt{\pi}\,(3\,s^2 - s\pi + q^2\pi^2)}, \tag{15}$$

can be expressed in terms of the heat capacities as

$$\chi_t = \frac{c_\phi}{c_q}\frac{\sqrt{s}}{\sqrt{\pi}} \tag{16}$$

Thermodynamics of RN-AdS black holes has been discussed extensively in [11] and [17]. There it was established that in the canonical ensemble these black holes show a liquid-gas like phase coexistence behaviour between a small black hole phase and a large black hole phase, culminating in a critical point of second order phase transition. However, in the grand canonical ensemble, they undergo a Hawking-Page phase transition to a thermal AdS space-time at low temperatures.

We shall briefly describe the phase behaviour in the different ensembles before proceeding to discuss the thermodynamic geometry of these black holes. As we have pointed out earlier, our presentation here is qualitatively different from that in the standard literature, and we find it more convenient to study the system using the parameters that will be used in the subsequent analysis of thermodynamic geometry for these black holes.

In the canonical ensemble the internal energy is allowed to fluctuate while the electric charge is held fixed, so that the black hole remains in thermal equilibrium with the heat reservoir held at a constant temperature t. This ensemble is aptly described by the Hehlmoltz potential

$$f(t,q) = m - t\,s = \frac{1}{4}\,\frac{3\,\pi^2 q^2 + \pi\,s - s^2}{\sqrt{s}\pi^{3/2}} \tag{17}$$

The variables (t, q) in the argument of f indicate the "control" parameters for the canonical ensemble, which can be tuned independent of each other. In the grand canonical ensemble however the charge is unconstrained and the black hole is in a thermal as well as electrical equilibrium with its reservoir held at a constant temperature t and a potential ϕ. The Gibbs free energy for this ensemble is

$$g(t,\phi) = m - ts - \phi q = -\frac{1}{4}\,\frac{\pi^2 q^2 - \pi\,s + s^2}{\sqrt{s}\pi^{3/2}} \tag{18}$$

where (t, ϕ) indicate the independent control parameters for this ensemble, even though we have expressed it in terms of s and q.

In order to describe the phase behaviour in the two ensembles we first present the relations between q and s obtained by solving for the divergences in the heat capacities. For the divergence in c_q the electric charge may be expressed as an implicit function of s as,

$$q_1(s) = \frac{\sqrt{s(\pi - 3\,s)}}{\sqrt{3}\pi} \quad , \tag{19}$$

whereas, along the divergence of c_ϕ, we obtain

$$q_2(s) = \frac{\sqrt{s(\pi - 3\,s)}}{\pi} \tag{20}$$

The stable and the unstable regions in the canonical ensemble are separated by the locus of the divergences of the heat capacity c_q while those in the grand canonical ensemble are separated by the divergences of the heat capacity c_ϕ. In fig.(1) we plot the curves $q_1(s)$ (red) and $q_2(s)$ (blue) in the q-s plane. The heat capacities c_q and c_ϕ are negative inside and positive outside their respective curves. We shall refer to the stability curve corresponding to the canonical ensemble as the c_q-spinodal curve and the one corresponding to the grand canonical ensemble as the c_ϕ-spinodal curve. The black curve representing $t = 0$ separates the naked singularity region on the left from the physical region on the right. Expectedly,

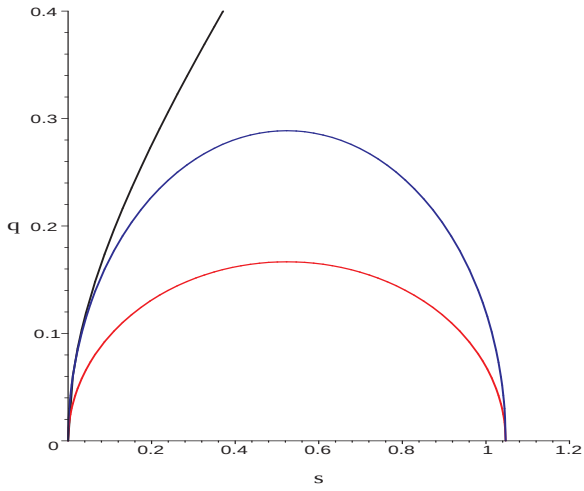

Figure 1: Stability curves of RN-AdS black holes. Heat capacities c_q and c_ϕ diverge along the upper blue and the lower red semi circular curves respectively. The extremal curve is black colored.

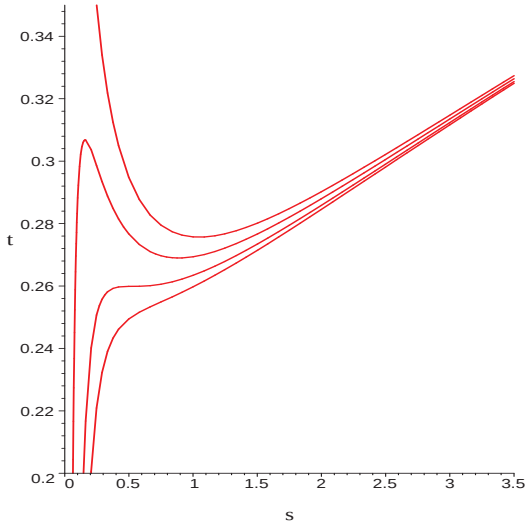

Figure 2: Isocharge plots of t vs. s with $q = 0$, 0.12, 0.167 (q_c), and 0.19 from the top to bottom. The critical isocharge curve in the middle shows an inflection at $s_c = \pi/6$ and $t_c = \sqrt{3}/\sqrt{2}\pi$

the canonical ensemble being the more constrained one, has a greater region of stability than the grand canonical ensemble.

From fig.(1) we can deduce the phase coexistence behaviour in the canonical ensemble as follows. Any constant q line intersects the c_q-spinodal curve twice for $q < q_c(= 1/6)$, thereby separating the small black hole branch from the large black hole branch by an unstable branch. This phase coexistence behaviour terminates at the critical charge, $q_c = 1/6$, where the constant q line becomes tangent to the c_q-spinodal curve, thus effecting a continuous second order phase transition between the small black hole and the large black hole. We shall discuss the critical exponents for the black hole in a canonical ensemble in brief in a later section where we present the critical behaviour for other ensembles.

In fig.(2) we present isocharge plots in the t-s plane for various fixed values of charge. The $q = 0$ curve at the top, corresponding to the AdS-Schwarzschild black hole, is characterized by a finite temperature minima or a turning point, below which there is no black hole solution and above which the unstable and stable branches coexist at all temperatures. We shall term this phase behaviour as "Davies" phase behaviour and the turning point temperature as the Davies temperature, t_d. This phase behaviour will turn out to be quite generic, as will be seen in later sections. Addition of a constant charge q causes a low temperature small black hole branch to form, or, in other words, it causes a "deconfinement" at all temperatures, [11]. On increasing the charge to q_c, the t-s curve shows an inflection at the critical point.

We now turn our attention to the black hole in a grand canonical ensemble, which is the one relevant for analysis in the framework of the thermodynamic geometry. In this ensemble the thermal AdS space with a constant pure gauge

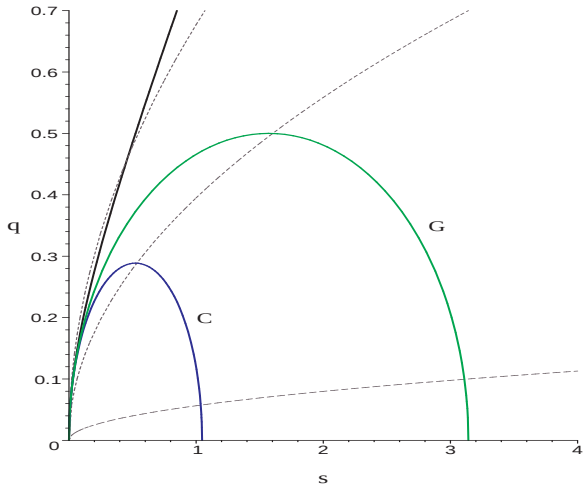

Figure 3: RN-AdS plots showing c_ϕ-spinodal curve in blue, zeroes of Gibbs free energy in green and isopotential curves in dotted grey at $\phi = 0.1$, 0.7, and 1.2 from bottom to top. Extremal curve is black in color..

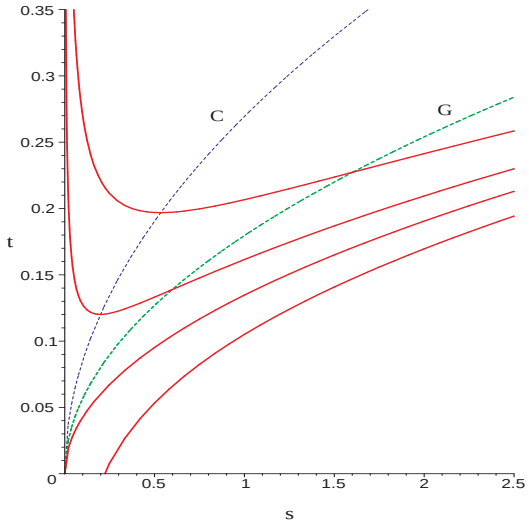

Figure 4: Plot showing isopotential curves in the $t - s$ plane of the RN-AdS black holes with $\phi = 0.7$, 0.9, 1 and 1.1 from top to bottom. The dotted green curve and dotted blue curve above it are the Gibbs and c_ϕ curves of fig.(3).

potential equal to that of the RN-AdS black hole can serve as a reference background (i.e, the zero of the Gibbs potential) since it is also a solution to the Einstein equations, ([11], [16], [17]). Therefore, while for negative values of g the black holes are globally stable, for positive values of g, they become unstable to the formation of thermal AdS via a Hawking-Page transition. The locus of zeroes of the Gibbs potential in the q-s plane can be obtained from the relation

$$q_3(s) = \frac{\sqrt{s\,(\pi - s)}}{\pi} \tag{21}$$

It will also be convenient to express the temperature as a function of s and ϕ using eqs. (10) and (12).

$$t = \frac{1}{4}\,\frac{\pi + 3\,s - \pi\,\phi^2}{\sqrt{s}\pi^{3/2}} \tag{22}$$

Using this expression for the temperature it may be verified that the extremal black holes exist only for $\phi \geq 1$. Eliminating q from eq.(12) and eq.(21) and then using eq.(22), the Hawking-Page phase transition temperature may be expressed in terms of the potential ϕ as

$$t_{hp} = \frac{\sqrt{1 - \phi^2}}{\pi} \tag{23}$$

In fig.(3) we show the grand canonical stability curve, i.e the c_ϕ spindodal curve, together with the green coloured "Gibbs curve" representing the zeroes of the

Gibbs potential. The two curves are labelled as "C" and "G" respectively. The three grey dotted curves represent isopotential curves, with the topmost one at a value of ϕ greater than one. In the region bounded by the Gibbs curve, the black hole is unstable against AdS as its free energy is positive. Since the c_ϕ-spinodal curve lies fully inside the Gibbs curve, we can say that the locally unstable black hole solutions are also always globally unstable. Thus we see that in the region bounded by the c_ϕ curve the black hole solutions exist but they are unphysical, whereas in the region lying in between the c_ϕ curve and the Gibbs curve metastable black holes exist. Outside the Gibbs curve , the black holes are both locally as well as globally stable. In fig.(4), we show isopotential plots in red of t vs. s for increasing values of ϕ from top to bottom, with the green dotted curve and the blue dotted curve being the Gibbs curve and the c_ϕ-spinodal curve respectively of fig.(3). For the top two isopotentials, having $\phi < 1$, the temperature shows a turning point when the isopotentials cross the c_ϕ curve. This is exactly the Davies phase transition behaviour mentioned earlier in the context of AdS-Schwarzschild black holes. The turning point temperature or the Davies temperature t_d, can be obtained in terms of the potential ϕ by eliminating s from eq.(12) and eq.(20), and then using eq.(22),

$$t_d = \frac{\sqrt{3}}{2}\,\frac{\sqrt{1-\phi^2}}{\pi} = \frac{\sqrt{3}}{2}\,t_{hp} \tag{24}$$

Thus, for $\phi < 1$, only the thermal AdS exists for $0 < t < t_d$, while a metastable black hole exists along with thermal AdS for $t_d < t < t_{hp}$. For $t > t_{hp}$ the stable black hole is preferred over the thermal AdS space-time. The lowest isopotential in fig.(4) is a typical one with $\phi > 1$, for which there is only a single black hole branch which is locally as well as globally stable at all temperatures. The extremal entropy for these isopotentials can be obtained from eq.(22), as

$$s_{ex}(\phi) = \frac{1}{3}\,\pi\,\left(\phi^2 - 1\right) \tag{25}$$

For $\phi = 1$ the black hole has a vanishing entropy at zero temperatures. Having discussed the phase behaviour of RN-AdS black holes in terms of the parameters suitable for describing the geometry of their equilibrium state space, we now turn to the discussion of the latter.

2.3 State Space Scalar Curvature for RN-AdS Black Holes

In this subsection, we will investigate the phase behaviour of RN-AdS black holes using thermodynamic geometry. The topic of thermodynamic geometry is by now well known, and we refer the reader to [8] for a comprehensive review, and to [10] for the details relevant to black hole thermodynamics. The thermodynamic line element for the RN-AdS black holes is a dimensionless quantity symbolically expressed as

$$dl^2 = g_{\mu\nu}dx^\mu dx^\nu = g_{mm}dm^2 + 2g_{mq}dmdq + g_{qq}dq^2, \tag{26}$$

where the indices μ, ν in the metric $g_{\mu\nu}$ range over the rescaled variables m and q. We note that thermodynamic geometry cannot be meaningfully defined in regions

of the equilibrium state space where the thermodynamic line element is negative, as the interpretation of the thermodynamic length between two neighbouring states as the measure of the probability of thermal fluctuation between them would then break down. The constraint of a positive definite line element requires that the deteminant formed by the metric $g_{\mu\nu}$ as well as its prinicipal minor, g_{mm} in this case, be positive definite, [8]. This is the familiar Le Chatelier's condition for local thermodynamic stability. It can be verified that this condition is satisfied for all regions lying outside the c_ϕ-spinodal curve in fig.(3), i.e, in regions where the black hole is locally stable.

The state space scalar curvature pertaining to the thermodynamic geometry for the RN-AdS black holes, first calculated in [18], is re-expressed in the scaled thermodynamic variables as

$$R = \frac{-9s\,(3\,s^2 + q^2\pi^2)\,(s^2 - s\pi + q^2\pi^2)}{(-3\,s^2 - s\pi + q^2\pi^2)\,(3\,s^2 - s\pi + q^2\pi^2)^2} \tag{27}$$

In what follows, we will elucidate novel interpretations of the curvature in terms of its zeroes and divergences in relation to the spinodal curves alluded to earlier. The analysis that follows from this perspective is entirely new and provides interesting insights into the behaviour and significance of the state space scalar curvature. We begin by noting that the curvature can be symbolically written in the following suggestive manner

$$R = -9s\left(3\,s^2 + q^2\pi^2\right)\frac{\mathcal{N}(g)}{\mathcal{N}(t)\mathcal{D}(c_\phi)^2} \tag{28}$$

where the symbols $\mathcal{N}(g)\,\mathcal{N}(t)$ and $\mathcal{D}(c_\phi)$ represent the numerators of the Gibbs potential and the temperature, and the denominator of c_ϕ respectively. This clearly shows that R diverges at extremality and along the c_ϕ-spinodal curve, both of which are at the boundary of the thermodynamically stable physical region. Interestingly, it goes to zero along the "Gibbs curve" of fig.(3) and has opposite sign of the Gibbs free energy everywhere. Let us see if we can substantiate this.

Note that the fact that R diverges along the c_ϕ-spinodal curve is quite reasonable as the scalar curvature pertains to the two dimensional state space Riemannian geometry which is directly related to the fluctuations in both the thermodynamic variables m and q. This would imply that R inherits the instabilities of the grand canonical ensemble, as reflected in its divergence along the c_ϕ-spinodal curve. In fact, a similar argument can explain the divergence at extremality, where the heat capacity changes sign on crossing to the unphysical naked singularity region. However, we believe that the issue of extremality in thermodynamic geometry is subtle and we will ignore this divergence in our future discussions.

Since R naturally describes the phase behaviour in the grand canonical ensemble, it would be convenient to re-express it in terms of the potential ϕ and t. To that end, we first express R in terms of ϕ and s, using eq.(12) and eq.(27), as follows:

$$R(\phi, s) = -9\,\frac{\pi^2\phi^4 - \pi^2\phi^2 + 4\,\pi\,\phi^2 s - 3\,\pi\,s + 3\,s^2}{(\pi\,\phi^2 - \pi - 3\,s)\,(3\,s + \pi\,\phi^2 - \pi)^2} \tag{29}$$

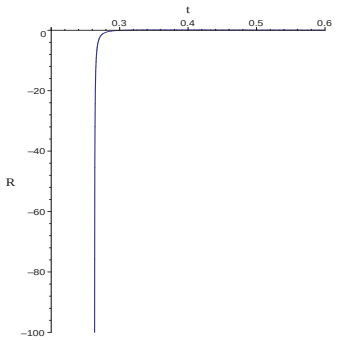

Figure 5: Isopotential plot of R vs. t with ϕ fixed at 0.03. R has a negative divergence at $t_b = 0.263$

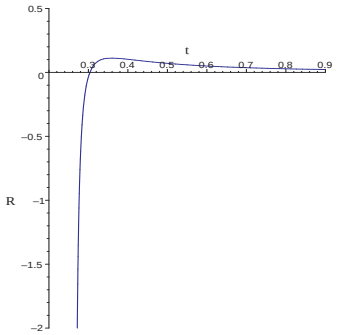

Figure 6: Close-up of fig.(5). R crosses zero and becomes positive at the Hawking-Page temperature $t_{hp} = 0.304$.

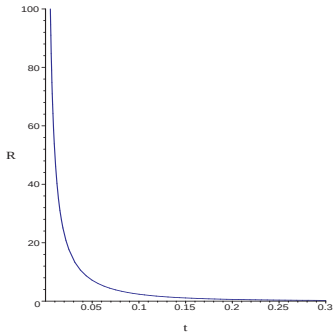

Figure 7: Isopotential plot of R vs. t with ϕ fixed at 1.3. R diverges at t=0 and remains positive at all t.

Solving eq.(10) for the entropy in terms of temperature, we obtain two solutions corresponding to the stable branch and the unstable branch. The stable branch solution is

$$s = \frac{1}{3}\,\pi\,\phi^2 - \frac{1}{3}\,\pi + \frac{4}{3}\,t\left(\frac{2}{3}\,t\pi^{3/2} + \frac{1}{3}\,\sqrt{4\,t^2\pi^3 + 3\,\pi\,\phi^2 - 3\,\pi}\right)\pi^{3/2} \tag{30}$$

On substituting the expression for s from eq.(30) into eq.(29) we obtain an expression for R for the positive-definite region in terms of ϕ and t as

$$R(\phi,t) =$$

$$\frac{9}{4}\,\frac{\phi^2\left(18\phi^2 + 48t^2\pi^2 - 27 + 18\pi tu\right) - 42\pi^2t^2 - 15t\pi u + 32t^4\pi^4 + 16\pi^3t^3u + 9}{\pi^2t\left(2\pi t + u\right)\left(3\phi^2 - 3 + 4\pi^2t^2 + 2t\pi u\right)^2} \tag{31}$$

where the expression u is given by

$$u = \sqrt{4\,\pi^2t^2 + 3\,\phi^2 - 3}$$

We now investigate R, as obtained in eq.(31), graphically by plotting R vs. t for various potentials. These plots pertain to the RN-AdS black hole in a grand canonical ensemble. Fig.(5) is a generic plot of R vs. t at a potential $\phi < 1$, and fig.(6) is a close-up of the same near the zero crossing of R. We clearly see that R shows a negative divergence at the Davies temperature t_d, eq.(24), corresponding to the turning point of the isopotential plots like the ones shown in fig.(4).

The scalar curvature remains negative for the metastable phase of the black hole, changing sign to positive at the Hawking-Page temperature t_{hp}, eq.(23). Fig.(7) shows a generic R vs. t plot for RN-AdS black holes with $\phi \geq 1$. From fig.(4) it can be seen that these black holes exist at all temperatures and are locally

as well as globally stable. The curvature mirrors this by remaining positive at all temperatures. Further, it can be seen from eq.(31) that for all values of the potential, in the limit of large t, R asymptotes to zero from the positive side as,

$$R \sim \frac{1}{t^2} \tag{32}$$

Eq. (31) and the analysis presented thereafter are the main results of this subsection. We will have more to say about the issue of sign of the state space curvature for RN-AdS black holes once we have discussed the phase behaviour and thermodynamic geometry for the Kerr-AdS black holes, to which we presently turn.

3 Kerr-AdS Black Holes

In this section, we begin by reviewing certain aspects of the thermodynamics of Kerr-AdS black holes, before we discuss the geometry of the equilibrium state space of the same. As earlier, our analysis will be directly in terms of the thermodynamic parameters which are relevant for the analysis of the state space geometry. The Kerr-Ads black holes are thermodynamically characterized by their mass and the angular momentum. On setting q=0 in eq.(4) we obtain the rescaled Smarr relation for the Kerr-AdS black hole as,

$$m = \frac{1}{2}\left(\frac{s^2\pi^2 + 4\,\pi^4 j^2 + 4\,j^2\pi^3 s + 2\,s^3\pi + s^4}{s\pi^3}\right)^{\frac{1}{2}} \tag{33}$$

The temperature, t, and the angular velocity, ω, are obtained by differentiating the expression for mass or equivalently by setting $q = 0$ in the corresponding formulae for the KN-AdS black holes in section (2.1).

The condition for extremality obtained by setting the numerator of t to zero leads to,

$$j_{ex}(s) = \frac{s}{2\pi^2}\,(\pi^2 + 4\,\pi\,s + 3\,s^2)^{1/2} \tag{34}$$

We note that the angular velocity ω that enters into the thermodynamics through the differentiation of the Smarr formula is not identical to the angular velocity at the horizon, ω_h. Instead, it turns out to be the difference in the angular velocity at horizon and that at the boundary of the spacetime, $\omega = \omega_h - \omega_\infty$, [16],[1] This also turns out to be the angular velocity of the rotating Einstein universe existing at the boundary of the asymptotically AdS space-time. This agrees well with the AdS/CFT picture and also shows that consistent thermodynamics up to infinity can be defined only when $\omega < 1$. A useful quantity for our calculations in Kerr-AdS case is the expression relating j to ω and s

$$j(\omega, s) = \frac{1}{2}\,\frac{\omega s^{3/2}\sqrt{\pi + s}}{\pi^{3/2}\sqrt{\pi + s - \omega^2 s}} \tag{35}$$

[1] i.e, it is measured with respect to a non-rotating frame at infinity, [24].

The expressions for the heat capacities at constant j and constant ω are lengthy, so we shall just write down the stability conditions corresponding to these heat capacities. The canonical ensemble stability constraint is obtained from the locus of the divergences of the specific heat c_j,

$$j_1(s) = \frac{s}{2\pi^2} \frac{(\pi + s)^{1/2}(-3\,\pi^2 - 9\,\pi\,s + 2\,Y - 6\,s^2)^{1/2}}{(3\,\pi + 4\,s)^{1/2}} \tag{36}$$

where Y is given by the expression

$$Y = (3\,\pi^3 + 10\,s\pi^2 + 15\,s^2\pi + 9\,s^3)^{1/2}(\pi + s)^{1/2} \tag{37}$$

Similarly, the stability condition for the grand canonical ensemble is obtained form the divergences of the heat capacity c_ω,

$$j_2(s) = \frac{s}{2\pi^2}\,(\pi + s)^{1/2}(2\,s^{1/2}\sqrt{\pi + s} - \pi - s)^{1/2} \tag{38}$$

Just like in the RN-AdS case, the Kerr-AdS black hole in the grand canonical ensemble also has a well defined reference background in the rotating thermal AdS with a zero Gibbs potential and angular velocity equal to that of the boundary angular velocity of the Kerr-AdS spacetime. For positive values of the free energy, the rotating thermal AdS space is more stable then the Kerr-AdS black hole, while the stability is reversed via a Hawking-Page phase transition when the free energy changes sign and becomes negative. The Gibbs free energy in the grand canonical ensemble may be obtained through the relation

$$g = m - ts - \omega j \tag{39}$$

It can be checked that the locus of the Hawking -Page phase transitions, or the zeroes of g are provided by the implicit relation

$$j_3(s) = \frac{s}{2\pi^2}\,(s^2 - \pi^2)^{1/2} \tag{40}$$

Now, keeping in mind that the thermodynamic geometry analysis will pertain to the grand canonical ensemble, we express the temperature t and the Gibbs free energy g in terms of ω and s by making use of eq.(35). These expressions turn out to be

$$t(\omega, s) = \frac{1}{4}\,\frac{\pi^2 + 4\,\pi\,s - 2\,\pi\,\omega^2 s + 3\,s^2 - 3\,\omega^2 s^2}{s^{1/2}(\pi + s)^{1/2}(\pi + s - \omega^2 s)^{1/2}\pi^{3/2}} \tag{41}$$

$$g(\omega, s) = \frac{1}{4}\,\frac{\sqrt{s}\,(\pi^2 + \omega^2 s^2 - s^2)}{\sqrt{\pi + s}\sqrt{\pi + s - \omega^2 s}\pi^{3/2}} \tag{42}$$

Eliminating s from eq.(42) and eq.(41), we obtain the Hawking-Page temperature as a function of ω,

$$t_{hp} = \frac{1}{2\pi}\,\frac{(1 + A + 2\,\sqrt{A})}{(\sqrt{A} + 1)} \tag{43}$$

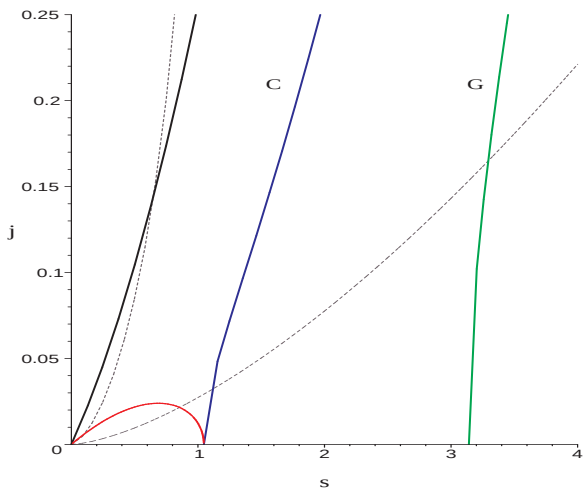

Figure 8: Kerr-AdS plots in s-j plane. From left to right in order are the black extremal curve, red semi circular c_j-spinodal curve, the blue c_ω-spinodal curve and the green Gibbs curve. Two grey dottted isopotentials have ω=0.3 (lower) and ω=1.9 (upper).

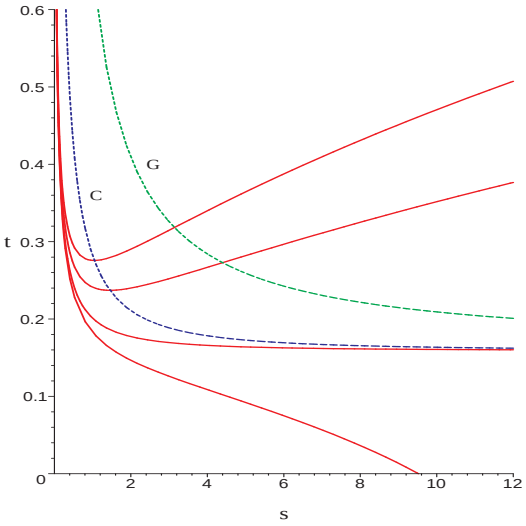

Figure 9: t vs. s plots for Kerr-AdS black holes showing isopotential curves in red colour, with the angular velocity ω ranging from 0, 0.7, 1 and 1.1 in order from top to bottom. The dotted green curve and dotted blue curve below it are the Gibbs and c_ω curves of fig.(8).

where $A = 1 - \omega^2$.

In fig.(8) we plot the the extremal curve, the stability curves and two isopotential curves using eq.(34), eq.(36), eq.(38), and eq.(35). The black line is the extremal curve, to the left of which lies the naked singularity region. The blue line, labelled as "C", is the grand canonical stability curve (or the c_ω-spinodal curve), to the right of which the heat capacity c_ω is positive. The right most green curve, labelled as "G", is the Hawking-Page curve, to the right of which the Gibbs energy of the black hole becomes negative. The small semi-circular red curve connecting the extremal curve and the c_ω-spinodal curve is the canonical stability curve or the c_j curve, below which the heat capacity c_j is negative. The canonical ensemble displays a liquid-gas like phase behaviour similar to the RN-AdS case, [16], where, for $j < j_c = 0.0239$, the Kerr-AdS black hole undergoes a first order transition between its small black hole and the large black hole phase. At the critical point j_c, which is the maxima of the c_j-spinodal curve, the constant j line in fig.(8) becomes tangent to the c_j-spinodal curve. The two dotted grey isopotential curves in fig.(8) have been obtained using eq.(35). The lower curve is a generic one for $\omega < 1$ while the upper one is a typical curve with $\omega > 1$.

In order to investigate the grand canonical ensemble more closely in fig.(9) we plot some isopotential curves (red in colour) in the s-t plane using eq. (41). The blue-dotted and the green-dotted curve above it are the c_ω-spinodal curve and the Gibbs curve respectively of fig.(8). The black hole is globally stable above the dotted green curve while it is locally unstable below the dotted blue curve. For $\omega < 1$ the black holes exhibit a typical Davies phase behaviour . The Davies

temperature can be obtained by substituting the expression for j from eq.(38) into the expression for temperature

$$t_d = \frac{1}{2}\,\frac{2\,\pi\,\sqrt{\pi+s}+3\,\sqrt{\pi+s}s-\pi\,\sqrt{s}}{\sqrt{3\,s+4\,\pi}\sqrt{\sqrt{s}+2\,\sqrt{\pi+s}s^{3/4}\pi}} \tag{44}$$

The black hole remains metastable between the temperatures t_d and t_{hp}, with the rotating thermal AdS being the preferred solution as it has a lower free energy. Beyond the Hawking-Page transition temperature the Kerr-AdS black hole becomes globally stable. Notce that the ω=1 isopotential curve asymptotes to the line $t = 1/2\pi$ from below, whereas the c_ω curve and the Gibbs curve asymptotes to this line from above, as s tends to infinity. This clearly shows that for $\omega \geq 1$ the Kerr-AdS black hole is both locally as well as globally unstable at all temperatures.

3.1 Scalar curvature of Kerr-AdS Black Holes and its Comparison with RN-AdS.

We now proceed to discuss the thermodynamic geometry of the Kerr-AdS black holes by first writing down the metric in the equilibrium state space in terms of the relevant thermodynamic variables j and m both of which are allowed to fluctuate. The line element in the state space with the usual significance is

$$dl^2 = g_{\mu\nu}dx^\mu dx^\nu = g_{mm}dm^2 + 2g_{mj}dmdj + g_{jj}dj^2, \tag{45}$$

The scalar curvature pertaining to the state space metric is a lengthy expression. We can write it down symbolically as

$$R = \frac{\mathcal{P}_{Kerr}}{\mathcal{N}(t)\mathcal{D}(c_\omega)^2} \tag{46}$$

where $\mathcal{P}_{kerr}$ is a polynomial expression of more than 30 terms and of degree 18 in s and 8 in j. The symbols $\mathcal{N}$ and $\mathcal{D}$ represent the numerator and denominator respectively of their arguments. Just like the in RN-AdS case the scalar curvature encodes the divergences in the grand canonical ensemble of the Kerr-AdS black hole. A salient difference with the RN-AdS black hole is that the curvature never crosses to the positive side and asymptotes to zero from the negative side as t tends to infinity. This is apparent from fig.(10) where the locus of zeroes of scalar curvature (marked as "R") is shown to lie to the left of the c_ω-spinodal curve and hence in the unstable region of the black hole. Thus, in the case of the Kerr-AdS black holes the state space scalar curvature carries no signature of a Hawking-Page phase transition. Substituting the expression for j from eq.(35) into the expression for the curvature we can obtain R as a function of ω and s. With a similar expression for t in terms of ω and s from eq.(41) we can obtain the asymptotic behaviour of R in terms of t,

$$R \sim -\frac{1}{t^4} \tag{47}$$

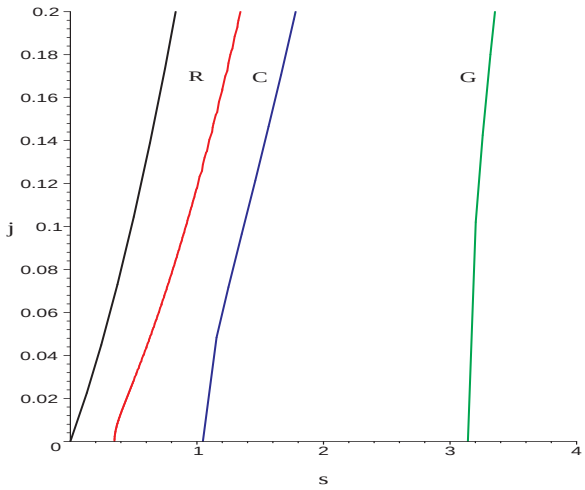

Figure 10: Kerr-AdS plots in the q-j plane. From left to right in order are the black extremal curve, zeroes of R in red, and the blue and green c_ω and the Gibbs curve respectively.

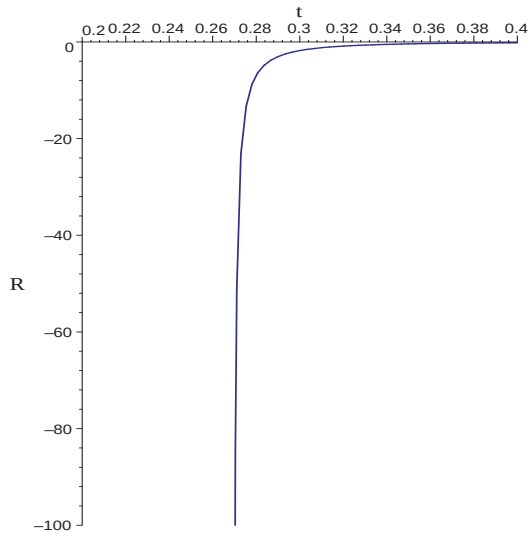

Figure 11: Isopotential plot of state space scalar curvature R vs. t for the Kerr-AdS black hole with ω fixed at a value of 0.3. R diverges at $t_2 = 0.269$ and remains negative at all t.

We should point out here that the exact significance of the sign of R is still an unsettled issue in the context of black holes.

Further exploring the behaviour of the scalar curvature in the RN-AdS and the Kerr-AdS black holes we now go to the AdS-Schwarzschild limit of both the black holes *via* their respective grand canonical ensembles, i.e, by setting their respective potentials, ϕ or ω, to zero. This ensures that the fluctuations in the respective charges, q or j, are still non-zero and hence a thermodynamic geometry analysis may be undertaken. Besides, it appears more natural to recover the AdS-Schwarzschild limit through the grand canonical ensemble of these black holes as there is no difference in the nature of the isopotential curves of fig.(4) or fig.(9), on setting ϕ or ω to zero. The AdS-Schwarzschild black holes continue to show a stable and an unstable branch starting at a turning point temperature and on further increasing the temperature undergo a Hawking-Page transition to a globally stable black hole On the other hand there is certainly a change in the isocharge curves when the charges q or j are set to zero in the canonical ensemble of RN-AdS (fig.(2)) or Kerr-AdS black holes. This is manifest in the disappearance of the small black hole branch.

The AdS-Schwarzschild limit of the scalar curvature is different in the two cases. For the RN-AdS black holes the curvature becomes

$$R_1 = -27\,\frac{s\,(\pi - s)}{(3\,s + \pi)\,(\pi - 3\,s)^2}, \quad q = 0 \tag{48}$$

For the Kerr-AdS black holes this limit becomes

$$R_2 = \frac{(\pi^2 - 3\,\pi\,s - 54\,s^2)\,\pi}{s\,(3\,s + \pi)\,(\pi - 3\,s)^2}, \quad j = 0 \tag{49}$$

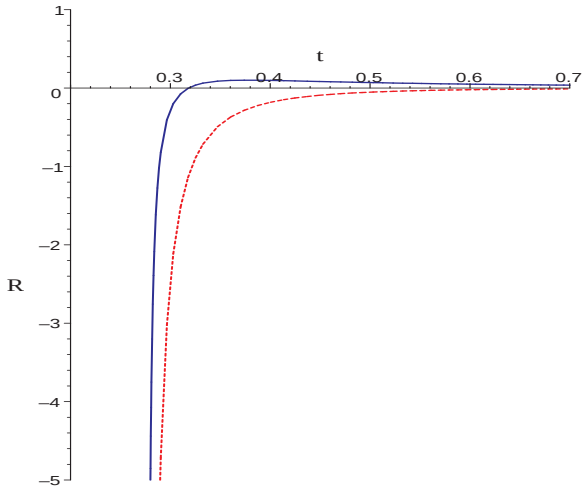

Figure 12: Zero potential plot of RN-AdS black hole in blue and the Kerr-AdS black hole in dotted red

In fig.(12) we plot the scalar curvature for the RN-AdS black hole in the grand canonical ensemble at zero potential vis a vis that of the Kerr-AdS black hole in the grand canonical ensemble at zero angular velocity. The zero potential RN-AdS curvature clearly encodes the Hawking-Page transition of the AdS-Schwarzschild black hole by crossing from negative to positive value at $t_{hp} = 1/\pi$. This is the main result of this subsection.

4 KN-AdS Black Holes in the Grand Canonical Ensemble

The thermodynamic behaviour of Kerr-Newman AdS black holes has been extensively discussed in [16] with reference to both the canonical and the grand canonical ensembles, whereas the thermodynamic geometry of these black holes has been discussed in details in our previous work [10]. Therefore we shall be brief in our discussions here and use the section mainly to compare the thermodynamic curvture of KN-AdS black holes with the RN-AdS and Kerr-AdS case.

Thermodynamic geometry is not applicable in the canonical ensemble for these black holes as both the charge and the angular momentum remain constrained with the mass as the only fluctuating thermodynamic variable, thereby rendering the thermodynamic metric trivial. However, we add that these black holes show interesting thermodynamic behaviour in the canonical ensemble, where, for a range of fixed charges q and j, they display a liquid gas like phase coexistence behaviour culminating in criticality much like in the canonical ensembles for RN-AdS and Kerr-AdS black holes. In the grand canonical ensemble all the three "charges" m , q, and j are unconstrained and the black hole is in a thermal, mechanical and electrical equilibrium with its reservoir held at constant temperature, electric potential and angular momentum respectively. The quantities t, ω and ϕ, which serve as control parameters for the grand canonical ensemble, have been obtained previously in terms of s, q and j by differentiating the scaled

Smarr relation, eq.(4). Using the expression for these conjugate variables, the heat capacity at constant potential and angular velocity, $c_{\phi\omega}$, and other susceptibilities may then be obtained. Referring the reader to the works mentioned at the beginning of this section for details, we now briefly describe the thermodynamic behaviour in the grand canonical ensemble. It will be convenient to express q and j in terms of the control parameters ϕ and ω by inverting eqs. (7) and (8).

$$\begin{aligned} q &= \frac{\phi\left[\pi s\left(\pi+s-\omega^2 s\right)\left(\pi+s\right)\right]^{\frac{1}{2}}}{\omega^2 s\pi-\pi s-\pi^2} \\ j &= \frac{\omega s^{\frac{3}{2}}\left(\pi\phi^2+s-\omega^2 s+\pi\right)\left[\left(s+\pi\right)\left(s+\pi-\omega^2 s\right)\right]^{\frac{1}{2}}}{2\pi^{\frac{3}{2}}\left(\omega^2 s-\pi-s\right)^2} \end{aligned} \tag{50}$$

Indeed, these expressions turn out to be useful since, using these, every other function like the temperature, Gibbs free energy, heat capacity or the state space scalar curvature may be re-expressed in terms of ϕ,ω and s, a form particularly suited to the grand canonical ensemble.

The thermal AdS space-time rotating with a fixed value of ω and at a constant pure gauge potential ϕ can serve as a reference background for the black holes in this ensemble, [16]. Therefore, when the Gibbs free energy of the black hole, defined as

$$g = m - ts - \phi q - \omega j \tag{51}$$

is positive, the rotating thermal AdS space-time is globally preferred while for negative g the black hole spacetime becomes more stable than AdS space. Setting $g(\omega, \phi, s)$ to zero we can obtain ϕ as an implicit function of ω and s. We call this function ϕ_1, where

$$\phi_1(\omega, s) = -\frac{\sqrt{-\pi^2 s-\pi^3+\omega^4 s^3-\pi\,\omega^2 s^2+s^2\pi+\pi^2\omega^2 s-2\,\omega^2 s^3+s^3}}{\sqrt{\pi}\sqrt{2\,\omega^2\pi\,s+\omega^2 s^2-s^2-2\,\pi\,s-\pi^2}} \tag{52}$$

Let us briefly recapitulate the phase behaviour for these black holes in the grand canonical ensemble. For $\omega, \phi < 1$ KN-AdS black holes exhibit a Davies phase behaviour similar to RN-AdS and Kerr-AdS in the grand canonical ensemble with their respective potentials less than unity. There are no black hole solutions up to the Davies temperature t_d, beyond which a locally stable and an unstable branch exist at all temperatures. For $t_d < t < t_{hp}$, the black hole remains in a metastable state. On further increasing the temperature to t_{hp} and above, the locally stable branch changes from metastable to globally stable via a Hawking-Page phase transition, as its Gibbs potential changes sign from positive to negative. For $\phi \geq 1$, $\omega < 1$ a globally as well as locally stable black hole branch exists at all temperatures, with an extremal solution at zero temperature. Along the divergence in $c_{\phi\omega}$ (i.e, setting the denominator of $c_{\phi\omega}$ to zero), we can express ϕ as follows

$$\phi_2(\omega, s) = \sqrt{\pi+s-\omega^2 s}\,\times$$

$$\frac{\sqrt{-3\,s^4\omega^4+6\,\omega^2s^4-3\,s^4-4\,\pi\,\omega^4s^3+12\,\pi\,\omega^2s^3-8\,s^3\pi+6\,\pi^2\omega^2s^2-6\,s^2\pi^2+\pi^4}}{\sqrt{\pi}\sqrt{s^4+\pi^4+4\,s^3\pi+4\,\pi^3s+6\,s^2\pi^2-4\,\pi^3\omega^2s-4\,\pi\,\omega^2s^3-6\,\pi^2\omega^2s^2-2\,\omega^2s^4+s^4\omega^4}} \tag{53}$$

For the case of $\omega \geq 1$ for which a globally as well as locally unstable branch exists at all temperatures [2] the thermodynamics is not consistently defined as the rotating Einstein universe at the boundary moves faster than light.

With the mass, charge and angular momentum all unconstrained the thermodynamic state space becomes three dimensional and the state space metric may be written as

$$g_{\mu\nu}(m,q,j) \equiv \begin{pmatrix} g_{mm} & g_{mq} & g_{mj} \\ g_{qm} & g_{qq} & g_{qj} \\ g_{jm} & g_{jq} & g_{jj} \end{pmatrix} \tag{54}$$

It can be verified that the line element corresponding to this metric is positive definite in regions where the heat capacity $c_{\omega\phi}$ is positive, [10]. Evidently, scalar curvature is not the only independent measure of curvature in three dimensions. However, following [15], where, for conventional thermodynamic systems, it was shown that in a higher dimensional state space R can still be associated with the correlation volume, we shall restrict our investigation to the state space scalar curvature only. The state space scalar curvature may be written symbolically as

$$R = \frac{\mathcal{P}_{KN}}{\mathcal{N}(t)\mathcal{D}(c_{\phi\omega})^2} \tag{55}$$

where $\mathcal{P}_{KN}$ is a lengthy polynomial expression of more than 300 terms and of degree $26, 24$, and 10 in s, q and j respectively. The divergence of R along the $c_{\phi\omega}$-spinodal "surface" in the s-q-j parameter space reflects the fact that the thermodynamic metric pertains to a grand canonical ensemble with all the thermodynamic variables set to fluctuate. Using the substitutions in eq.(8), the scalar curvature can be written in terms of ϕ, ω and s, which is in a form suited for analysis in the grand canonical ensemble.

The curvature has been studied in our previous work, [10], so we shall not elaborate on it in any detail. The general form of the R vs. t plots for $\phi < 1, \omega < 1$ and $\phi \geq 1, \omega < 1$ is the same as the corresponding plots for RN-AdS black holes, as shown in fig.(5), fig.(6) and fig.(7). However, now the zero crossing of R for the case $\phi < 1$ is no more at the same temperature as the zero crossing of the free energy. The presence of j fluctuations separates the zeroes of R ("the R curve") and the zeroes of Gibbs free energy, g.

Let us investigate this effect in more detail. In figs(13), fig.(14)and fig.(15) we plot the zeroes of R, the Gibbs curve and the $c_{\phi\omega}$-spinodal curve in the ϕ-s plane for different fixed values of ω in an increasing order from left to right. The first figure in the series has ω=0 and is an "RN-AdS" black hole in the grand canonical ensemble with a non zero fluctuation in j about a zero mean value. Whereas without the j fluctuations the zeroes of R and g would have coincided, now the two curves intersect each other at $\phi_0 \approx 0.82$ with an increasing separation for smaller values of ϕ. It can be verified that while for $\phi < \phi_0$ the

[2] for $\omega = 1$ the unstable branch exists for all t above a minimum value that depends on ϕ

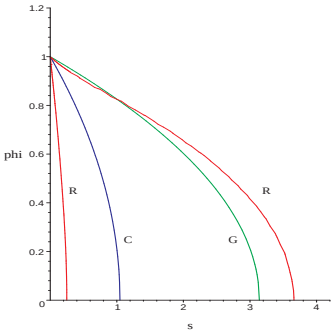

Figure 13: ϕ-s plot of infinities of $c_{\phi\omega}$ and zeroes of R and g, at $\omega = 0$.

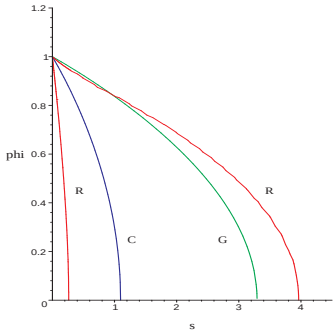

Figure 14: ϕ-s plot of infinities of $c_{\phi\omega}$ and zeroes of R and g, at $\omega = 0.3$

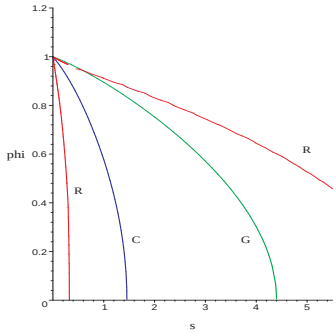

Figure 15: ϕ-s plot of infinities of $c_{\phi\omega}$ and zeroes of R and g, at $\omega = 0.7$.

scalar curvature crosses zero and becomes positive at a temperature, t_R above the Hawking-Page temperature t_{hp}, for $\phi > \phi_0$ it crosses zero at a temperature t_R which is slightly below the Hawking Page phase transition temperature t_{hp}. The qualitative pattern remains the same for higher values of ω, even though the separation between the R curve and the Gibbs curve at lower ϕ progressively increases. To get an idea of the order of difference in t_R and t_{hp} let us find them for two different ranges of ϕ and ω values. At the potentials $\omega = 0.9, \phi = 0.1$, for which the R-curve and the Gibbs curve are well separated according to the previous discussion, the two temperatures turn out to be $t_R = 0.309$ and $t_{hp} = 0.226$. Whereas, with $\phi = 0.9$, $\omega = 0.1$, for which the curves are nearly coincident, the temperatures turn out to be $t_R = 0.132$, $t_{hp} = 0.136$. Interestingly, for all ω there exists a $\phi = \phi_0$ for which the R curve and the Gibbs curve intersect, i.e, $t_R = t_{hp}$.

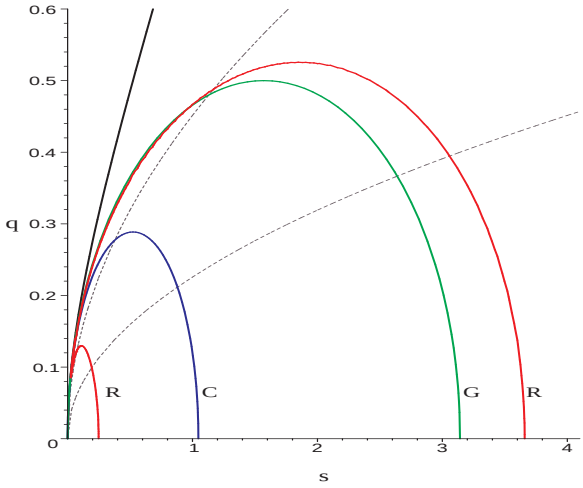

Figure 16: Plot of infinties of $c_{\phi\omega}$ and zeroes of R and g in the q-s plane at $j = 0$. Grey dotted isopotential curves are at $\phi = 0.4$ below and $\phi = 0.8$ above.

For a comparison with the RN-AdS black hole we redraw fig.(13) in the $j = 0$

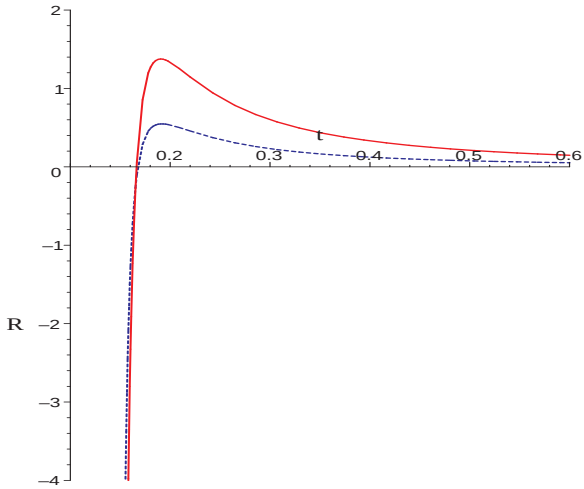

Figure 17: R vs t plot showing KN-AdS curvature in red at $\omega = 0, \phi = 0.85$ and RN-AdS curvature in dotted blue at $\phi = 0.85$

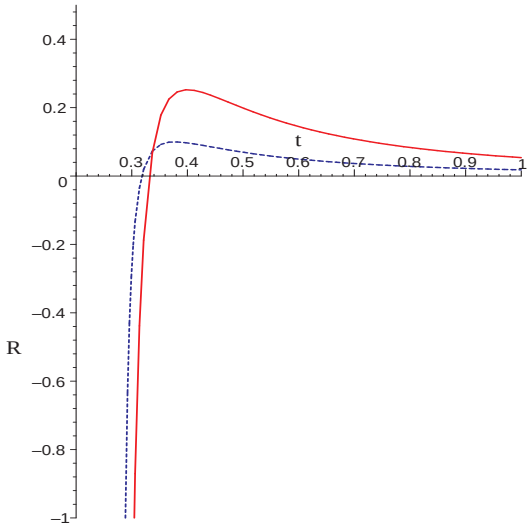

Figure 18: R vs t plot showing KN-AdS curvature in red at $\omega = 0, \phi = 0$ and RN-AdS curvature in dotted blue at $\phi = 0$.

section of the s-q-j parameter space to obtain fig.(16). The green Gibbs curve marked "G" and the blue $c_{\phi\omega}$-spinodal curve marked "C" are same as the curves in fig.(3) while the R-curve is marked in red. The small R-curve lies in the unstable region and so is irrelevant. Comparing fig.(3), where the R-curve coincides with the Gibbs curve, and fig.(16), we can make out the difference between the absence of j and finite fluctuations about a zero mean value of j. Two isopotentials in dotted grey have been shown for a correspondence with fig.(13). In fig.(17) we compare the R vs. t plot of the KN-AdS scalar curvature in its "RN-AdS" limit with the plot of the RN-AdS curvature, both of them at $\phi = 0.85$. Expectedly, given the large value of the potential, the two curvatures are very similar, with the zero of the KN-AdS curvature slightly different from the zero of RN-AdS curvature owing to j fluctuations.

We now take the "AdS-Schwarzschild" limit of the Kerr-Newman thermodynamic curvature by setting both q and j to zero in its expression. The corresponding black hole system is a KN-AdS black hole held at $\phi = \omega = 0$, because of which the mean values of j and q remain at zero, with non-zero fluctuations around the mean. The curvature turns out to be

$$R_3 = \frac{\pi^3 - 6\,s\pi^2 - 90\,s^2\pi + 81\,s^3}{s\,(3\,s+\pi)\,(\pi - 3\,s)^2} \tag{56}$$

The behaviour of R_3 is very similar to the RN-AdS curvature in the AdS-Schwarzschild limit, R_1, obtained in eq.(48) and shown in fig.(12). The zero crossing of R_3, however, is different owing to the j fluctuations, and takes place at $t_R = 0.331$ which is greater than the zero crossing of R_1 at $t_{hp} = 1/\pi = 0.318$. We show this in fig.(18), where the curvatures R_3 and R_1 have been plotted together for comparison.

For large temperatures R decays to zero in the same way as the RN-AdS black hole curvature, i.e, $R \sim 1/t^2$ as $t \to \infty$.

5 KN-AdS Black Holes in the Mixed Ensembles

The Kerr-Newman AdS black hole in the grand canonical ensemble has all its thermodynamic charges, m, j and q unconstrained. However, note that the electric charge, q, and the angular momentum, j, are quite unlike each other physically. It is therefore reasonable to consider ensembles with restricted fluctuations, in which one of the two thermodynamic charges, j or q, is held fixed, while the other fluctuates. We may term such ensembles as "mixed" ensembles, since the black hole can be said to be in a canonical ensemble with respect to the constrained charge, while it is in a grand canonical ensemble with respect to its fluctuating charge, which it exchanges with its surrounding at a constant conjugate potential. This would lead one to consider "mixed" susceptibilities like $c_{j\phi}$, the heat capacity at constant angular momentum and electric potential, and, similarly, $c_{q\omega}$ etc. For the case of the asymptotically flat Kerr-Newman black holes such mixed heat capacities were considered in [21], where their critical exponents were calculated, while [22] and [23] considered all possible thermodynamic fluctuations in these black holes with extensive discussions on their stability and thermodynamic geometry. KN-AdS black holes with restricted fluctuations were investigated extensively by us in a previous work, [10], where we had discussed their phase behaviour and certain aspects of thermodynamic curvature. It was observed that in the mixed ensemble the KN-AdS black holes posessed a rich phase structure, exhibiting liquid gas like phase coexistence regions and critical points. In the following we shall briefly outline the phase structure of these black holes from a somewhat new perspective, before proceeding to discuss their critical behaviour in the next section.

The fixed j-ensemble is formed by adding a constant angular momentum, j, to the RN-AdS black hole in a grand canonical ensemble. Since this black hole does not exchange its angular momentum j with the reservoir it is "mechanically" isolated, even though it continues to maintain an electrical equilibrium with its surroundings. The free energy for this ensemble is given by

$$A = m - ts - \phi q \tag{57}$$

where the conjugate quantities are now given by their full KN-AdS thermodynamic relations, eqs. (7), (8) and eq.(9). This free energy, "A", remains constant during a first order phase transition, exhibiting a multivalued branched structure or a swallow tail shape in a free energy vs. temperature plot. However, now the zeroes of the free energy do not correspond to a Hawking-Page phase transition. This is because thermal AdS with a fixed angular momentum, j, is no more a solution to the Einstein equations, and therefore cannot serve as a reference background in action calculation with fixed j and fixed ϕ boundary conditions. For more details we refer the reader to our previous paper [10] and the references therein.

In fig.(19) we pictorially depict the effect of adding constant j by drawing the stability curves in the three dimensional s-q-j parameter space. As j becomes

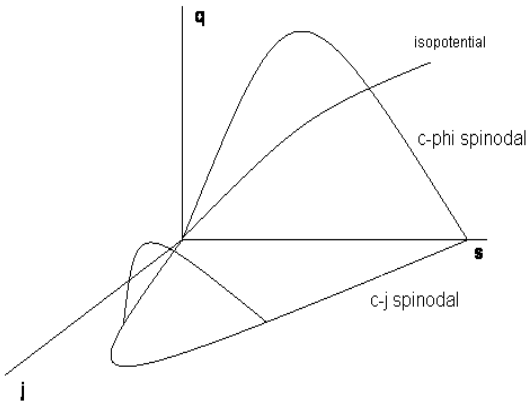

Figure 19: Picture showing the shifting of the c_ϕ spinodal curve along the c_j spinodal curve. Critical behaviour exists only up to the maxima of c_j curve at j_c=0.0239.

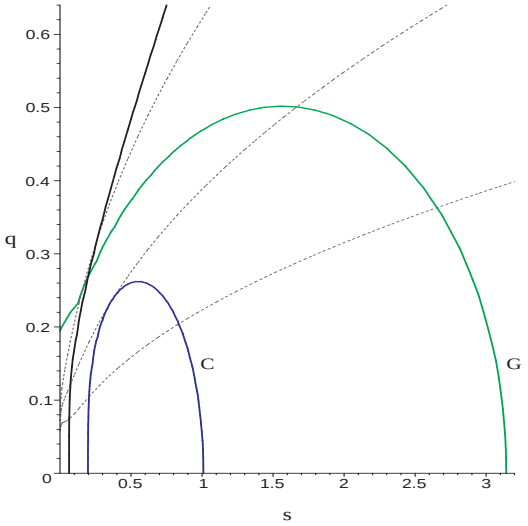

Figure 20: Plot of extremal, Gibbs and c_ϕ curves in the q-s plane for fixed j ensemble, with $j = 0.011$. Isopotential curves in dotted grey are at $\phi = 0.395, 0.687(\phi_c)$ and 1.1 from bottom to top.

non zero, the c_ϕ spinodal curve in the q-s plane of RN-AdS black hole begins to "slide" along the j axis in such a way that its base always lies on the c_j spinodal curve in the j-s plane of Kerr-AdS black hole. As a consequence of this, some amount of parameter space becomes available to the left of the (shifted) c_ϕ curve[3]. Therefore, now the isopotential plots can cut the c_ϕ curve *twice*, thus effecting an abrupt change from the Davies phase behaviour for $j = 0$ to a liquid-gas like phase behaviour with a small black hole branch and a large black hole branch. In fig.(20) we plot the c_ϕ stability curve in the q-s plane for a fixed j. We also plot the zeroes of the free energy, A, labelling it as the "G curve". A comparison of fig.(20) with fig.(1) for RN-AdS black hole clearly brings out the shifting of the "C" curve to the right as discussed above. Among the representative isopotentials shown in the figure, those that intersect the c_ϕ curve twice will have their t-s curves typically like those in fig.(2), with a first order transition between the small and the large black hole branches. The isopotential curve tangent to the c_ϕ curve becomes the critical curve, along which the black hole undergoes a second order phase transition at the tangent, which is therefore the critical point for a given value of j. For ϕ values beyond the critical potential the j-ensemble black hole changes continuously from the small black hole phase to the large black hole phase without undergoing any phase transition. Referring back to the pictorial depiction in fig.(19) we can infer that the c_ϕ curve eventually shrinks and disappears as it reaches the maxima of the c_j spinodal at $j = j_c = 0.0239$,

[3]More precisely, it is the constant j section of the $c_{j\phi}$ spinodal surface but we shall continue to name it as c_ϕ curve.

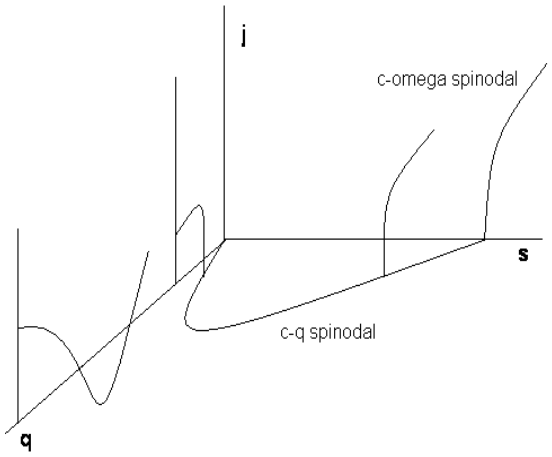

Figure 21: Picture showing the shifting of the c_ϕ spinodal curve along the c_j spinodal curve. Critical behaviour exists only up to the maxima of c_j curve at j_c=0.0239.

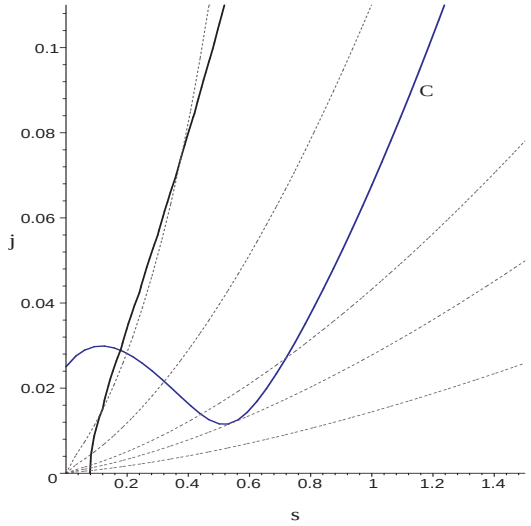

Figure 22: Plot showing the extremal curve and the c_ω curve in the q-ensemble, with $q = 0.17 > q_c$. The isopotentials are at $\omega = 0.15, 0.286(\omega_c), 0.74, 1, 2.12$ respectively from bottom to top

which is the critical point of the Kerr-AdS black hole in the canonical ensemble. For $j > j_c$ the black holes in the fixed j-ensemble has a unique stable branch at all temperatures.

The fixed q ensemble is similarly formed by adding a constant charge q to the Kerr-AdS black hole in a grand canonical ensemble, so that the black hole remains "electrically " isolated while continuing to maintain its mechanical equilibrium with the reservoir. The free energy for the q- ensemble is given as

$$B = m - ts - \omega j \tag{58}$$

where the conjugate potentials are once again given by eqs. (7), (8) and eq.(9). Similar to the j-ensemble this free energy exhibits a swallow tail shape in a first order transition. However, the q-ensemble has a richer phase behaviour than the fixed j ensemble, as we will show below.

In the three dimensional pictorial depiction of fig.(21) we can observe the effect of adding a constant q term. The c_ω curve in the j-s plane corresponding to the Kerr-AdS black hole translates along the c_q spinodal curve belonging to the RN-AdS black hole in the $s - q$ plane at the base. As a result of this an additional branch of c_ω curve appears to the left of the c_q curve, giving rise to a low temperature stable black hole branch separated from the stable large black hole branch by an unstable region. On further increasing the charge the two c_ω branches join together at the maxima of the c_q curve at $q = q_c = 1/6$, which is the critical point of the RN-AdS black hole in the canonical ensemble. Interestingly, up to $q = q_c$, there are no critical points, with a discontinuous phase transition between the small and the large black hole taking place for all values of angular

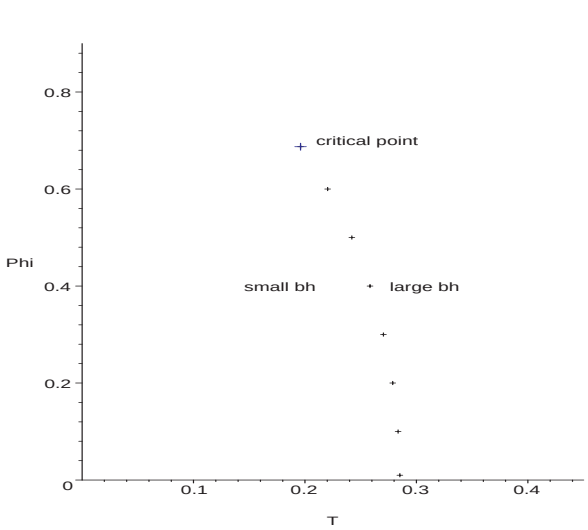

Figure 23: Phase coexistence curve in the ϕ-t plane of the $j = 0.011$ ensemble.

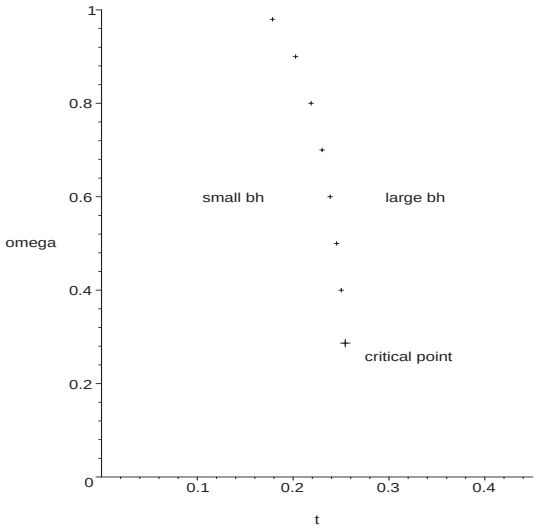

Figure 24: Phase coexistence curve in the ω-t plane of the $q = 0.17$ ensemble.

velocity less than unity[4] At the same time, for $q > q_c$, critical point exists for all values of q. In fig.(22), we look at the critical behaviour of the q-ensemble in a greater detail by plotting the c_ω curve in the j-s plane for a fixed q value greater than q_c. The heat capacity is positive below the c_ω curve. The critical isopotential curve, having angular velocity ω_c, is the one which is tangent to the c_ω stability curve. For $1 > \omega > \omega_c$ the black hole shows a liquid-gas like phase coexistence behaviour with a first order transition between the small black hole and the large black hole.

To end this subsection, we plot, in fig.(23), the coexistence curve in the ϕ-t plane for the fixed j ensemble. Notice the analogy with the liquid-vapour coexistence curve in the pressure-temperature plane $(p - t)$ for fluids, with the correspondence $\phi \leftrightarrow p$. The slope of the coexistence curve can be understood through the Clausius-Claperyon equation. At any point on the coexistence curve having co-ordinates (t, ϕ), the Gibbs free energies of the small black hole, A_1, and the large black hole, A_2, have the same value, *i.e* $A_1 = A_2$. On moving along the coexistence curve to a nearby point, $(t + \Delta t, \phi + \Delta\phi)$, the new free energies of the two branches will still be equal to each other, thus implying $\Delta A_1 = \Delta A_2$. Given that the variation in Gibbs free energy is given by $\Delta A = -s\Delta t - q\Delta\phi$ we obtain

$$-s_1\Delta t - q_1\Delta\phi = -s_2\Delta t - q_2\Delta\phi \tag{59}$$

where the subscripts 1 and 2 indicate the small black hole and the large black hole respectively. From this equation we obtain the slope of the coexistence curve as

$$\frac{\Delta\phi}{\Delta t} = -\frac{s_2 - s_1}{q_2 - q_1} \tag{60}$$

[4]For $\omega > 1$ there are no stable large black hole branches for any fixed q.

The slope of the coexistence curve is clearly negative here, while it is positive in the case of fluids because of the sign convention for pressure which treats the pressure applied *on* the fluid as positive.

For the fixed q-ensemble, the phase coexistence plot is shown in fig.(24). The slope is again negative, as can be verified by a calculation analogous to the one presented above. However, this has qualitatively different features from that of the fixed j-ensemble curve of fig.(23).

5.1 Critical exponents in the mixed ensembles

In systems exhibiting second order phase transitions the order parameter and various susceptibilities display a power law behaviour near the critical point. This is essentially because of the dominance near criticality of the long range correlated fluctuations, as a result of which the system description becomes scale invariant. The scaling exponents or the critical exponents for the power law dependence of these quantities are seen to be the same for a wide variety of systems. This feature of universality again follows from the divergence of the correlation length near the critical point, which renders the details of microscopic interactions irrelevant. In fact, the various systems can be classified under separate universality classes, based on the spatial dimension of the system and that of the order parameter. We will first list the critical exponents corresponding to various thermodynamic functions for the liquid gas system, as an example. The divergence of the specific heat at constant volume above and below the critical temperature goes as follows:

$$\begin{aligned} c_v &\sim (t_r)^{-\alpha} \\ c_v &\sim (-t_r)^{-\alpha'} \end{aligned} \tag{61}$$

where $t_r = \frac{t_c - t}{t_c}$. The isothermal susceptibility $\kappa_t = (\frac{1}{\rho}\frac{\partial \rho}{\partial p})|_t$ diverges as

$$\begin{aligned} \kappa_t &\sim (t_r)^{-\gamma} \\ \kappa_t &\sim (-t_r)^{-\gamma'} \end{aligned} \tag{62}$$

The order parameter, $\Delta\rho = \rho - \rho_{cr}$, varies along the coexistence curve as

$$\Delta\rho \sim (t_r)^{\beta} \tag{63}$$

where $(t < t_c)$. Finally, along the critical isotherm, the variation of the order parameter with its intensive variable is given as

$$\Delta\rho \sim (p_r)^{1/\delta}. \tag{64}$$

where $p_r = \frac{p_c - p}{p_c}$. The critical behaviour can be neatly summarized in the "static scaling hypothesis", which is one of the central results of renormalization group theory, [19], [20]. According to this, in the vicinity of the critical point, the singular part of the free energy is a generalized homogeneous function (GHF) of its variables. Thus, for a liquid gas system for example, we have

$$G_s(\lambda^{a_t}\Delta t, \lambda^{a_p}\Delta p) = \lambda G_s(\Delta t, \Delta p), \tag{65}$$

where Δt and Δp are deviations from their critical values and a_t and a_p are called the scaling powers of temperature and pressure. It then follows from the properties of GHFs that all the derivatives and Legendere transforms of the free energy will also be GHFs. The critical exponents $\alpha, \beta, \gamma, \lambda$, which can now be obtained by differentiating the fundamental equation (65), are seen to depend on *two* independent quantities a_t and a_p . This leads to two independent scaling relations between the exponents.

$$\begin{aligned} \alpha &+ 2\beta + \gamma = 2 \qquad \text{(Widom equality).} \\ \gamma &= \beta(\delta - 1) \qquad \text{(Rushbrooke equality).} \end{aligned} \tag{66}$$

Another consequence of eq. (65) is that the primed and unprimed exponents like α, α' and γ, γ' are the same. The critical exponents and scaling relations were first discussed in the context of Kerr-Newman black holes in [21], and were worked out in detail for RN-AdS black holes in [12]. As discussed previously, in both the 'q' and the 'j' ensembles the KN-AdS black holes exhibit a liquid gas like phase behaviour, with a typical liquid-vapour like coexistence curve culminating in a critical point (fig.(21)). We now discuss the critical exponents and scaling relations in these ensembles.

Since the expressions for thermodynamic functions are too lengthy and algebraically complicated, they cannot be inverted to obtain the equation of state which, in turn, may be used to calculate the exponents, as is the standard procedure.

These can, however, be obtained iteratively using an expansion of the thermodynamic quantities in the neighbourhood of the critical point in powers of the (small) path variable along which the critical point is approached. We shall describe this method using the constant j ensemble as a concrete example. Let us look at the scaling behaviour near critical point along the equipotential curves. For any two points (q, s) and $(q+\Delta q, s+\Delta s)$ lying on a curve of constant potential in the q-s parameter space, see fig.(20), the following relation will hold

$$\phi(q + \Delta q, s + \Delta s) = \phi(q, s) = \text{constant} \tag{67}$$

Since the motion is constrained on an equipotential curve, the variations of s and q are not independent of each other. With q chosen as the independent path variable, s now becomes an implicit function $s(q)$, whose form has to be determined iteratively. To this end, we write down a symbolic expansion of $s(q)$ as a power series in Δq around its value, $s(\tilde{q}) = \tilde{s}$, at an arbitrary point, $q = \tilde{q}$, on the equipotential curve.

$$s(\tilde{q} + \Delta q) - s(\tilde{q}) = \Delta s = s_1(\tilde{q})\Delta q + \frac{1}{2!}s_2(\tilde{q})(\Delta q)^2 + \frac{1}{3!}s_3(\tilde{q})(\Delta q)^3 + ... \tag{68}$$

The coefficients s_1, s_2, etc can now be obtained recursively from eq. (67) by first expanding $\phi(\tilde{q} + \Delta q, s(\tilde{q} + \Delta q))$ in a Taylor series in Δq and Δs about the point $(\tilde{q}, \tilde{s})$, then plugging in the expansion of Δs from eq. (68) and requiring that the final expression vanish at all orders Δq, Δq^2, etc. Thus, it can be verified that

$$
\begin{aligned}
s_1 &= -\frac{\phi_q}{\phi_s} \\
s_2 &= -\frac{1}{\phi_s^3}\left[\phi_{qq}\phi_s^2 - 2\phi_{qs}\phi_q\phi_s + \phi_{ss}\phi_q^2\right] \\
s_3 &= -\frac{1}{\phi_s^5}\left[\phi_{qqq}\phi_s^5 - 3\phi_{qqs}\phi_q\phi_s^3 + 3\phi_{qss}\phi_q^2\phi_s^2 - \phi_{sss}\phi_q^3\phi_s - 3\phi_{qs}\phi_{qq}\phi_s^3\right. \\
&\quad \left. +6\phi_{qs}^2\phi_s^2\phi_q - 9\phi_{qs}\phi_{ss}\phi_s\phi_q^2 + 3\phi_{ss}\phi_q\phi_{qq}\phi_s^2 + 3\phi_{ss}\phi_q^3\right] \qquad (69)
\end{aligned}
$$

where the symbol ϕ_s represents $\partial\phi/\partial s$ and ϕ_{sq} represents $\partial^2\phi/\partial s\partial q$, etc. Having obtained these coefficients we can now expand the temperature $t(q,s)$ near the critical point as a power series in the *order parameter* $\Delta q = q - q_{cr}$, by approaching the critical point along the critical curve $\phi(q,s) = \phi_{cr}$. [5] Using the coefficients from eq. (69), it can be verified that

$$
t(q_{cr} + \Delta q, s_{cr} + \Delta s) = t_{cr} + \frac{1}{3!}t_3(\Delta q)^3 + \text{ higher order terms}, \qquad (70)
$$

where t_3 is a positive constant of order unity whose exact value depends on the critical point. Similarly, it can be verified that the inverse of specific heat at constant potential, c_ϕ[6], goes as

$$
c_\phi^{-1}(q_{cr} + \Delta q, s_{cr} + \Delta s) = \frac{1}{2!}c_2(\Delta q)^2 + \text{ higher order terms}, \qquad (71)
$$

where c_2 is a positive constant. Further, one can check that the capacitance $\chi_t = (\partial q/\partial\phi)|_t$ also diverges in the same way as the specific heat.

$$
\chi_t^{-1} \sim (\Delta q)^2 \qquad (72)
$$

Thus, in order to find the scaling exponents for c_ϕ, for example, we can readily infer from eq. (70) and eq. (71) that

$$
c_\phi \sim (t_r)^{-3/2}. \qquad (73)
$$

A completely analogous calculation gives the scaling behaviour of various thermodynamic quantities along the critical isotherm, $t(q,s) = t_{cr}$. For this, we first rewrite eq.(67) along isotherms.

$$
t(q + \Delta q, s + \Delta s) = t(q,s) = \text{constant} \qquad (74)
$$

Proceeding in a similar manner, we obtain the coefficients corresponding to eq. (69)

$$
\begin{aligned}
s_1^{'} &= -\frac{t_q}{t_s} \\
s_2^{'} &= -\frac{1}{t_s^3}\left[t_{qq}t_s^2 - 2t_{sq}t_st_q + t_{ss}t_q^2\right] \qquad (75)
\end{aligned}
$$

[5] The critical points are obtained numerically owing to the inability to invert many of the algebraic expressions involved

[6] Here, c_ϕ is the restriction of $c_{j\phi}$ on constant j sections of the parameter space

with $s_3^{'}$ having a similar expression as s_3 of eq. (69), and as before, the symbol t_s, t_{sq} stand for $\partial t/\partial s$ and $\partial^2 t/\partial s \partial q$, etc. On plugging these coefficients into the expansion of $\phi(q,s)$ around the critical point, we can numerically verify that

$$\phi(q_{cr}+\Delta q, s_{cr}+\Delta s) = \phi_{cr} + \frac{1}{3!}\phi_3(\Delta q)^3 + \text{ higher order terms}, \tag{76}$$

where ϕ_3 is a positive constant whose value depends on the critical point. Similarly, it can be verified that along the critical isotherm, specific heat c_ϕ goes as

$$c_\phi^{-1}(q_{cr}+\Delta q, s_{cr}+\Delta s) = \frac{1}{2!}c_2^{'}(\Delta q)^2 + \text{ higher order terms}, \tag{77}$$

where $c_2^{'}$ is positive. Having elucidated our general approach, we now list out the critical exponents corresponding to both the ensembles.

For the fixed j ensemble we obtain

$$\alpha_j = 2/3, \quad \beta_j = 1/3, \quad \gamma_j = 2/3, \quad \delta_j = 3\ . \tag{78}$$

where the subscript j indicates the ensemble. Note that these exponents follow both the scaling relations eq. (66). Moreover, these exponents are exactly the same as the critical exponents for RN-AdS black holes in the canonical ensemble, [11] and [12]. [7]

The critical exponents for the q-ensemble can be obtained by a similar calculation. We first consider entropy as an implicit function $s(j)$ along the critical isopotential curve, $\omega(j,s) = \omega_{cr}$, or the critical isotherm, $t(j,s) = t_{cr}$, and then write down a symbolic expansion for it around the critical point in powers of the order parameter $\Delta j = j - j_{cr}$. The coefficients of expansion, obtained recursively just as in the j-ensemble, are then used to calculate various critical exponents. We list them here:

$$\alpha_q = 2/3, \quad \beta_q = 1/3, \quad \gamma_q = 2/3, \quad \delta_q = 3\ . \tag{79}$$

Which is exactly the same as in the fixed j ensemble, and again, these exponents follow both the scaling laws of eq. (66).

We are now in a position to make a very interesting observation. The fact that the critical exponents calculated in this subsection matches exactly with those for the RN-AdS black holes and the Kerr-AdS black holes (with appropriate identification of the thermodynamic parameters) indicates a kind of universality in the critical behaviour. Black holes being non extensive thermodynamic systems, thermodynamic behaviour of these are ensemble dependent. However, for critical points in different ensembles, the KN-AdS black hole seems to have an universal set of critical exponents, irrespective of the ensemble chosen.

The calculation of the critical exponents for the KN-AdS black holes, together with the observation made in the last paragraph constitute the main results of this subsection. In the last subsection, we briefly comment on scaling relations of the Ruppeiner curvature for the mixed ensembles.

[7] the critical exponents of Kerr-AdS black holes in the canonical ensemble, which we have checked independently, are the same as RN-AdS exponents

5.2 Scalar curvature for KN-AdS Black Holes in the Mixed Ensembles

The state space scalar curvature R for the constant j and constant q ensembles can be symbolically expressed as

$$R_j = \frac{\mathcal{P}_j}{s\mathcal{N}(t)\mathcal{D}(c_\phi)^2} \quad ; \quad R_q = \frac{\mathcal{P}_q}{s\mathcal{N}(t)\mathcal{D}(c_\omega)^2} \tag{80}$$

where the symbols $\mathcal{N}$ and $\mathcal{D}$ represent the numerator and denominator respectively of their argument, and $\mathcal{P}_j$ is a polynomial of about 250 terms while $\mathcal{P}_q$ is a polynomial of about 200 terms. Here the subscripts j and q are used to label the ensembles. We observe that R diverges along the spinodal curve (which includes the critical point) and the extremal curve. As discussed in [10], inside the coexistence region bounded by the spinodal curve the line element of the corresponding state space scalar curvature is negative, and hence thermodynamic geometry is not applicable in that region. Similarly, the extremal curve separates the physical region from the naked singularity region where thermodynamic geometry is once again not applicable owing to a negative line element in the corresponding state space.[8] We will mainly be interested in the divergence of R at criticality. Before we pass on to discuss the behaviour of scalar curvature near the critical point, we note the following observation at extremality. For both the "mixed" ensemble black holes considered, the product of the scalar curvature and the specific heat at fixed charge has a limiting value of unity at $t = 0$. Thus, for the j ensemble, we have

$$\lim_{t\to 0} R_j c_q = 1 \quad , \tag{81}$$

where R_j is the scalar curvature at fixed j and c_q is the restriction of the specific heat c_{jq} on the constant j section. Similarly, for the fixed q ensemble we obtain

$$\lim_{t\to 0} R_q c_j = 1 \quad . \tag{82}$$

where R_q is the scalar curvature at fixed q and c_j is the restriction of the specific heat c_{jq} on the constant q section. This agrees with the result obtained in [22] for asymptotically flat black holes. As was observed in [10], R always shows a negative divergence at the critical points of both the q and the j ensembles. This is similar to its behaviour in conventional systems displaying criticality. Moreover, the denominator of R_j contains the square of the denominator of c_ϕ or $(\partial q/\partial\phi)|_t$) and that of R_q contains the square of the denominator of c_ω or $(\partial j/\partial\omega)|_t$). That R shares its divergence with specific heat at constant potential or with the susceptibilities is not unexpected as its calculation envisions the black hole in a grand canonical ensemble, with the relevant charges fluctuating.

In conventional thermodynamic systems the state space scalar curvature is interpreted as a correlation volume ξ^d, where ξ is the correlation length and d

[8] The thermodynamics at extremality is more subtle as it is governed by quantum fluctuations and not thermal fluctuations. Like the previous cases we shall ignore the divergences near extremality.

is the spatial dimension of the system, [8]. We may define a critical exponent ϑ corresponding to the scaling of R as

$$R \sim t_r^{-\vartheta} \tag{83}$$

Using the critical exponent for the correlation length,

$$\xi \sim (t_r)^{-\nu} \tag{84}$$

and the hyperscaling relation, ([8], [19], [20]),

$$d\nu = 2 - \alpha \qquad \text{Josephson equality} \tag{85}$$

we can write down the scaling relation for ϑ as

$$\vartheta = 2 - \alpha \qquad \text{Ruppeiner equality} \tag{86}$$

where we have termed the scaling relation for curvature as "Ruppeiner equality". Using eq. (73) and eq. (86), it can be further verified that

$$R c t_r^2 = K \quad , \tag{87}$$

where c is the specific heat capacity and K is a constant having dimensions of entropy. Using "two scale factor universality" (see references in [8]) the constant term K can be seen to be a combination of critical exponents,

$$K = -\beta(\delta - 1)(\beta\delta - 1)\kappa_B \tag{88}$$

Thus, the r.h.s of eq. (87) is a universal constant in a given equivalence class of critical exponents. On putting in the values of critical exponents for different universality classes, it can be verified that K is in general negative, which in turn implies that R is negative near the critical point.

However, in the case of black holes, as observed in [22], the state space scalar curvature is a dimensionless number as opposed to its dimension of volume in conventional thermodynamic systems. Besides, there is no interpretation of a correlation length as such for black holes. Thus, R can no longer be interpreted as a correlation volume. Nevertheless, with the understanding that it is a measure of "correlations" at the horizon, [22], we can still continue to investigate its scaling behaviour near criticality. Recalling the observation that R contains the square of the denominator of specific heat at constant potential we can write down its scaling beahviour as

$$R_j \sim t_r^{-2\alpha_j} \quad ; \quad R_q \sim t_r^{-2\alpha_q} \tag{89}$$

where the subscripts indicate constant q or constant j ensemble. Recalling from eqns (78) and (79) that $\alpha_j = \alpha_q = 2/3$, it can be verified that the scaling relation for ϑ, eq.(86), still holds in spite of the Josephson equality not being a meaningful one in the context of black holes. Similarly, the validity of eq.(86) also ensures that eq.(87) too holds in the case of the mixed ensemble black holes. Thus, close to the critical point

$$R_j\, c_\phi\, t_r^2 = K_j \quad , \quad R_q\, c_\omega\, t_r^2 = K_q \tag{90}$$

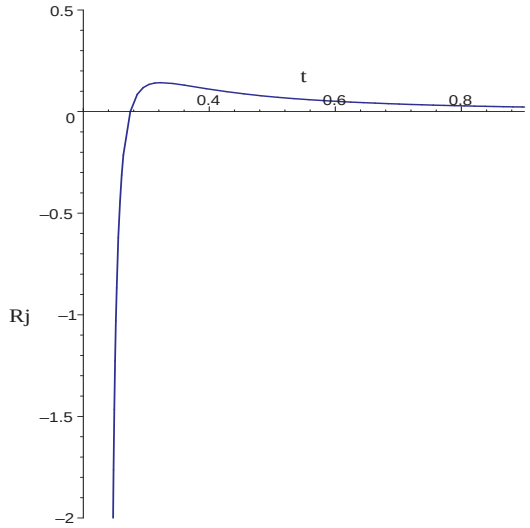

Figure 25: Plot of R_j vs. t for the large black hole phase along an isopotential curve, $\phi = 0.5$. j is fixed at a value of 0.011.

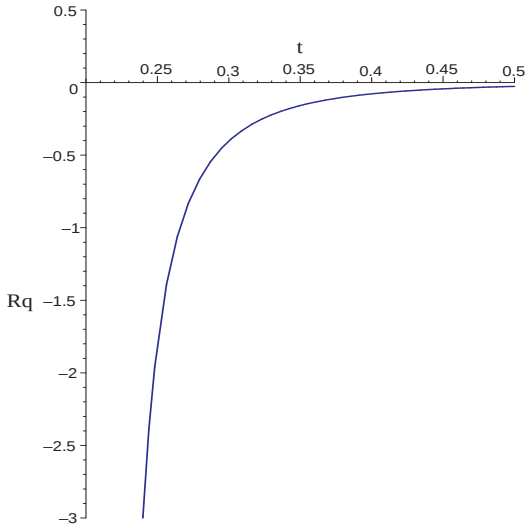

Figure 26: Plot of R_q vs. t for the large black hole phase along an isopotential curve, $\omega = 0.8$. q is fixed at a value of 0.16.

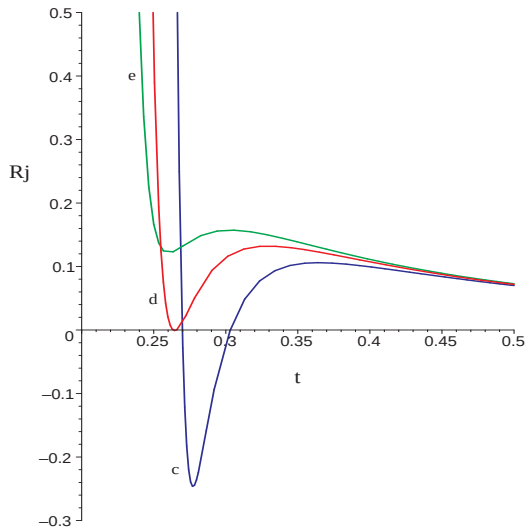

Figure 27: Plot of R_j vs. t along isopotential curves with $\phi_c = 0.12$, $\phi_d = 0.4$, $\phi_e = 0.5$. j is fixed at a value of 0.043.

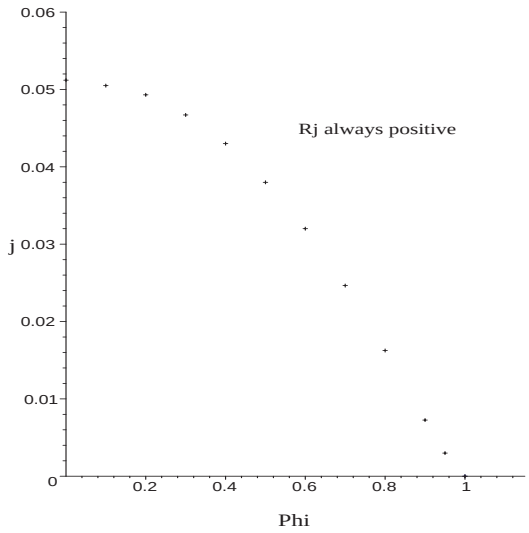

Figure 28: Locus of points in the j-ϕ plane above which $R > 0$ for all t. The curve intersects the j axis at $j = 0.0512$.

However, the constants K_j and K_q do not follow eq.(88) as "two scale factor universality" is not valid for black holes. We add that, as observed in [10], R is always negative in the critical region.

Let us now discuss the behaviour of R for large black holes in the two mixed ensembles. In fig.(25) and fig.(26) we show generic plots of R_j vs t and R_q vs t respectively in the large black hole phase. It can be seen from the figures

that while in the j-ensemble the state space scalar curvature always changes sign from negative to positive on increasing the temperature, in the q-ensemble the curvature corresponding to the large black hole phase remains negative at all temperatures. These figures are similar to figs. (1a) and (2a) for the RN-AdS and Kerr-AdS black holes respectively. In both cases we can see from eq. (80) that the state space scalar curvature asymptotes to zero as s, and therefore t, tends to infinity. However, it can be verified that, they do so from opposite sides of the t-axis. For large t, their asymptotic behaviour becomes

$$R_j \sim \frac{1}{t^2} \quad , \quad R_q \sim -\frac{1}{t^4} \tag{91}$$

Notice that the asymptotic behaviour remains the same as the RN-AdS and Kerr-AdS black hole, *i.e*, the $j = 0$ or the $q = 0$ case respectively. These observations lead us to conclude that while the constrained, non fluctuating charges have a decisive role to play in the thermodynamics of small black holes at low temperatures, they do not play a significant role in the thermodynamics of high temperature large black holes. It also serves to re-emphasize the different nature of q and j fluctuations, as was noticed previously.

We can make a further observation for the constant j black holes in relation to the sign of R. Fig.(29) shows a plot of R_j vs. t for three isopotential curves, with its angular momentum j fixed at a value of 0.043. The black hole does not exhibit criticality since its angular momentum is above the critical value $j_c = 0.0239$, fig.(2a). However, on following the behaviour of R along the isopotential curves ϕ_c, ϕ_d, and ϕ_e we notice that there is a "critical" value of $\phi = \phi_d$ beyond which R remains positive at *all* temperatures. This is similar to the case of $\phi > 1$ for RN-AdS black holes, shown in fig.(7). In fig. (30) we plot a locus of such "critical" points in the j-ϕ plane. From the figure it can also be inferred that there is a minimum value of the fixed angular momentum, $j = j_p = 0.0512$, above which the scalar curvature remains positive at all temperatures for any value of the potential ϕ.

Finally, continuing our investigation of the sign of R in the j ensemble we now focus our attention on the comparison between the zeroes of the scalar curvature and the zeroes of the free energy. We recall that in the case of RN-AdS black holes (*i.e*, "$j = 0$" ensemble) the zeroes of R and the free energy coincide. Let us see how a non-zero j effects a change in this. In each of the figs. (6), (7) and (8), which are labeled by increasing values of j from left to right, we represent the zeroes of curvature by the red curve and those of the free energy by the green curve while zeroes of the temperature are represented by the black extremal curve. The scalar curvature is negative under the curve of its zeroes and positive outside while the free energy is positive under its curve and negative outside. The naked singularity region lies to the left of the extremal curve. On comparing these figures with fig.(3) for RN-AdS black holes we can infer that introduction of a non-zero *constant* j causes a separation of the zeroes of R and the free energy. On increasing the value of j, the R curve shrinks, thus widening the gap with the free energy curve, until it would finally disappear at $j = 0.0512$, fig.(30). Notice that the pattern of separation of the R curve and the G curve is different from the case of *fluctuating* j, as shown in fig.(16) and in fig.(13) to fig.(15) of section

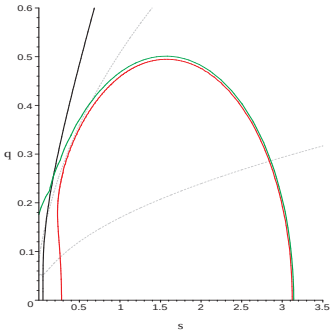

Figure 29: Locus of zeroes of R, t and the free energy for $j = 0.009$. Grey dotted isopotentials are at $\phi = 0.3$ below and $\phi = 0.9$ above.

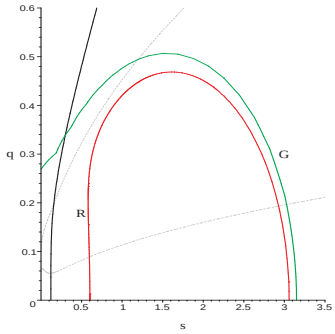

Figure 30: Locus of zeroes of R, t and the free energy for $j = 0.021$. Grey dotted isopotentials are at $\phi = 0.2$ below and $\phi = 0.8$ above

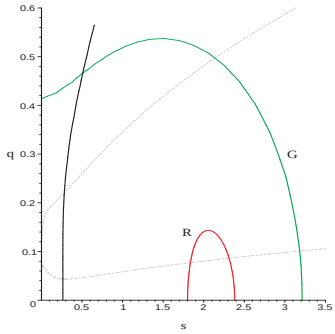

Figure 31: Locus of zeroes of R, t and the free energy for $j = 0.0497$. Grey dotted isopotentials are at $\phi = 0.1$ below and $\phi = 0.6$ above

5. In the former, constant case, the R curve is always inside the G curve, while in the latter, fluctuating case, the R curve lies on both sides of the G curve. Again, in the constant j case, for each fixed j below $j_p = 0.0512$ there always exists a minimum ϕ above which R never crosses zero and is always positive, as mentioned in the preceding paragraph. Beyond j_p, R is positive for all ϕ. In comparison, in the fluctuating j case, R always crosses zero for all $\phi < 1$. Moreover, in the latter case, for higher values of ϕ the R curve and the G curve are almost coincident. It should be borne in mind, however, that in the mixed ensemble, the zeroes of Gibbs potential do not have the interpretation of a "Hawking-Page" curve.

6 Discussions and Conclusions

In this paper, we have studied various aspects of criticality, scaling behaviour, and thermodynamic geometry of AdS black holes, following our earlier work in [10]. This completes the comprehensive analysis of the structure of the equilibrium thermodynamic state space geometry of AdS black holes. Several observations leading to important new insights regarding the phase structure of these black holes have been obtained in this context. The methods used in this analysis are significantly different from the ones conventionally used in the literature. The critical exponents for second order phase transitions in the mixed ensembles introduced and elucidated in [10] for the KN-AdS black holes have also been calculated. These have been compared to the critical exponents for RN-AdS and Kerr-AdS black holes in the canonical ensemble and are found to be identical. This suggests an universality in critical phenomena for AdS black holes.

The state space scalar curvature involving fluctuations in all the thermodynamic variables have been studied in the grand canonical ensemble for KN-AdS black holes. Our results establish the significant fact that the fluctuations in the electric charge and those in the angular momentum are distinctly different from each other in their respective effects on the geometry of the thermodynamic state

space. One of the main conclusions of this analysis is that for black holes whose state space geometry involves electric charge fluctuations exhibits a change in sign of the scalar curvature, which closely parallels the corresponding change in sign of the Gibbs free energy. In fact, remarkably for the RN-AdS black holes, we establish an exact correspondence between the zeroes of the state space scalar curvature and that of the Gibbs free energy. It turns out that for the range of parameters for which the black hole is globally stable against thermal AdS, the scalar curvature is positive and is negative when the black hole is globally unstable. However interestingly, for the Kerr-AdS black holes, this phenomenon is notably absent and the scalar curvature remains negative at all temperatures. Also, for the case of the fixed j mixed ensemble, we have established a minimum value of the potential ϕ above which the scalar curvature is positive at all temperatures.

In order to further explore the effect of fluctuations on the sign of the scalar curvature, we have considered the full set of fluctuating thermodynamic charges in the case of the KN-AdS black hole in the grand canonical ensemble. The effect of fluctuations in the angular velocity and the electric potential on the sign of the curvature have been studied in details in this context. The significant outcome of this analysis is that a close correspondence between the zeroes of the curvature and the Gibbs free energy is observed only at large values of the electric potential. Further, the RN-AdS limit of the KN-AdS scalar curvature was also studied, leading to the observation that the fluctuations in the angular momentum j causes a shift in the zeroes of the state space scalar curvature. The asymptotic behaviour of the thermodynamic scalar curvature was also studied, illustrating significant differences between the RN-AdS and the Kerr-AdS black holes.

Finally, we have studied the behaviour of the thermodynamic curvature of KN-AdS black holes in the mixed ensembles near criticality, and obtained a hyperscaling relation. Interestingly, this behaviour closely resembles that of conventional thermodynamic systems. This provides further justification for using thermodynamic geometry as an effective tool for analysing phase transitions and critical phenomena in black hole thermodynamics.

It would be interesting to apply our formulation to analyse black hole thermodynamics in higher derivative gravity theories. This may lead to interesting phase structures and corresponding critical phenomena for these systems. The same is true for higher dimensional AdS black holes. Further, the significance of the novel phase behaviour of KN-AdS black holes in the mixed ensembles established and elucidated by us in this paper and our earlier work [10], vis a vis the AdS/CFT correspondence, is an interesting open problem for the future.

References

[1] R. M. Wald, "The thermodynamics of black holes," Living Rev. Rel. **4**, 6 (2001) [arXiv:gr-qc/9912119].

[2] D. N. Page, "Hawking radiation and black hole thermodynamics," New J. Phys. **7**, 203 (2005) [arXiv:hep-th/0409024].

[3] R. Brout, S. Massar, R. Parentani and Ph. Spindel, "A Primer for Black Hole Quantum Physics," Phys. Rept. **260**, 329 (1995) [arXiv:0710.4345 [gr-qc]].

[4] O. Aharony, S. S. Gubser, J. M. Maldacena, H. Ooguri and Y. Oz, "Large N field theories, string theory and gravity," Phys. Rept. **323**, 183 (2000) [arXiv:hep-th/9905111].

[5] L. Tisza, "Generalized Thermodynamics," Pub. MIT Press, Cambridge, MA (1966)

[6] H. B. Callen, "Thermodynamics and an Introcution to Thermostatitics," Pub. Wiley, New York (1985)

[7] F. Weinhold, J. Chem Phys. **63** (1075) 2479, *ibid* J. Chem Phys. **63** (1975) 2484.

[8] G. Ruppeiner, Rev. Mod. Phys. **67** (1995) 605, erratum *ibid* **68** (1996) 313.

[9] S. Ferrara, G. W. Gibbons and R. Kallosh, "Black holes and critical points in moduli space," Nucl. Phys. B **500**, 75 (1997) [arXiv:hep-th/9702103].

[10] A. Sahay, T. Sarkar and G. Sengupta, "Thermodynamic Geometry and Phase Transitions in Kerr-Newman-AdS Black Holes," [arXiv:1002.2538 [hep-th]].

[11] A. Chamblin, R. Emparan, C. V. Johnson and R. C. Myers, "Charged AdS black holes and catastrophic holography," Phys. Rev. D **60**, 064018 (1999)

[12] X. N. Wu, "Multicritical Phenomena Of Reissner-Nordstrom Anti-De Sitter Black Holes," Phys. Rev. D **62**, 124023 (2000).

[13] H. Janyszek, R. Mrugala, "Geometrical Structure of the State Space in Classical Statistical and Phenomenological Thermodynamics," Rep. Math. Phys. **27** (1989) 145.

[14] B. Mirza and H. Mohammadzadeh, "Ruppeiner Geometry of Anyon Gas," Phys. Rev. E **78**, 021127 (2008) [arXiv:0808.0241 [cond-mat.stat-mech]].

[15] G. Ruppeiner "Riemannian geometric approach to critical points: General theory", Phys. Rev. **E 57** (1997) 5135.

[16] M. M. Caldarelli, G. Cognola and D. Klemm, "Thermodynamics of Kerr-Newman-AdS black holes and conformal field theories," Class. Quant. Grav. **17**, 399 (2000) [arXiv:hep-th/9908022].

[17] A. Chamblin, R. Emparan, C. V. Johnson and R. C. Myers, "Holography, thermodynamics and fluctuations of charged AdS black holes," Phys. Rev. D **60**, 104026 (1999) [arXiv:hep-th/9904197].

[18] J. E. Aman, I. Bengtsson and N. Pidokrajt, "Geometry of black hole thermodynamics," Gen. Rel. Grav. **35**, 1733 (2003) [arXiv:gr-qc/0304015].

[19] H. E. Stanley, "Scaling, universality, and renormalization: Three pillars of modern critical phenomena," Rev. Mod. Phys. **71**, S358 (1999).

[20] Scaling, Universality and Renormalization Group Theory, M.E Fisher.

[21] C. O. Lousto, "The Fourth law of black hole thermodynamics," Nucl. Phys. B **410**, 155 (1993) [Erratum-ibid. B **449**, 433 (1995)] [arXiv:gr-qc/9306014].

[22] G. Ruppeiner, "Stability And Fluctuations In Black Hole Thermodynamics," Phys. Rev. D **75**, 024037 (2007).

[23] G. Ruppeiner, "Thermodynamic curvature and phase transitions in Kerr-Newman black holes," Phys. Rev. D **78**, 024016 (2008) [arXiv:0802.1326 [gr-qc]]. [arXiv:hep-th/9902170].

[24] G. W. Gibbons, M. J. Perry and C. N. Pope, "The first law of thermodynamics for Kerr - anti-de Sitter black holes," Class. Quant. Grav. **22**, 1503 (2005) [arXiv:hep-th/0408217].